GDP-9

LIQUEFACTION POTENTIAL OF COHESIONLESS SOILS

GEOTECHNICAL DESIGN PROCEDURE

GDP-9

Revision #3

AUGUST 2015

NEW YORK STATE OF OPPORTUNITY. Department of Transportation | Office of Technical Services | Geotechnical Engineering Bureau

GEOTECHNICAL DESIGN PROCEDURE:
LIQUEFACTION POTENTIAL OF COHESIONLESS SOILS

GDP-9
Revision #3

STATE OF NEW YORK
DEPARTMENT OF TRANSPORTATION

GEOTECHNICAL ENGINEERING BUREAU

AUGUST 2015

ABSTRACT

This report provides basic knowledge about liquefaction of cohesionless soils under seismic loading. Presented also are the most widely accepted methods for evaluating the liquefaction potential of cohesionless oils in level ground, for estimating earthquake-induced settlements and for analyzing slope stability against flow slides. Sample problems to demonstrate each design procedure are included in the appendices.

A brief review is presented of the seismicity of New York State, the level of which can be characterized as moderate. The State historically has experienced earthquakes up to a magnitude of 6.0. Earthquakes of this magnitude can cause structural and ground failures from liquefaction. Liquefaction-induced failure types and factors affecting liquefaction susceptibility are also reviewed.

Finally, methods for improving in-situ soil conditions to reduce liquefaction susceptibility are discussed.

TABLE OF CONTENTS

LIST OF FIGURES

FIGURE **PAGE**

LIST OF TABLES

TABLE **PAGE**

1. INTRODUCTION

1.1 Purpose

The purpose of this report is to provide basic knowledge about liquefaction of cohesionless soils under seismic loading for NYSDOT Geotechnical Engineering Bureau designers, and secondly, to present the most widely accepted methods for evaluating the liquefaction potential of soils, for analyzing stability of embankments and slopes against flow failures resulting from liquefaction and for estimating the earthquake-induced settlements in cohesionless soil deposits. Due to the complex nature of the subject and the fact that controversies concerning liquefaction still exist, this report may be subject to revision as new design procedures or consensus become available. Interested readers may refer to publications by Seed (1979), Finn (1981), Ishihara (1985), National Research Council (1985) and Castro (1987).

1.2 General

A number of failures of embankments, natural slopes, earth structures and foundations have been attributed to the liquefaction of sands caused by either static or seismic loading. Case histories of landslides or flow failures due to liquefaction are the 1937 Zeeland coast of Holland slides involving 7 million cubic meters of alluvial sands, and the 1944 Mississippi River slide near Baton Rouge containing about 4 million cubic meters of fine sands. Failures of hydraulic fill dams such as the Calaveras Dam in California in 1918, the Fort Peck Dam in Montana in 1938, and the Lower San Fernando Dam during the 1971 San Fernando Earthquake in California, just to name a few, were triggered by the liquefaction of sands. Although the importance of liquefaction of sands induced by static loading has been recognized since the work of Casagrande (1936), the subject of liquefaction of sands by seismic loading had not received a great deal of attention until 1964 when two major earthquakes shook Anchorage, Alaska, and Niigata, Japan, resulting in substantial damage and loss. The Alaska earthquake in 1964, a shock with a magnitude, M, of 9.2 on the Richter scale, destroyed or damaged more than 200 bridges and caused massive landslides. During the 7.5-magnitude earthquake of June 16, 1964, in Niigata, Japan, the extensive liquefaction of sand deposits resulted in major damage to buildings, bridges, highways and utilities. It was estimated that more than 60,000 buildings and houses were destroyed.

To date, after 30 years of intensive research on this subject, much progress has been made in understanding the liquefaction phenomena of cohesionless soils under seismic loading. A variety of methods for evaluating the liquefaction potential of soils have been proposed.

New York State generally is not as seismically active as states that have areas located near tectonic plate boundaries. The probability of the State being struck by a major earthquake is small. However, historical records indicate that New York State has experienced M=4 to 6 earthquakes, which can produce ground shaking levels up to VIII on the Modified Mercalli Intensity, MMI (For definitions of MMI and Richter magnitudes, see Appendix A). Earthquakes of this intensity can cause liquefaction resulting in structural and ground failures.

1.3 Liquefaction Phenomena

The liquefaction phenomenon of soil deposits can be described as the reduction of shear strength due to pore pressure buildup in the soil skeleton. The shear strength of cohesionless soil, τ, depends mainly on the angle of internal friction and the effective stress acting on the soil skeleton and can be

expressed as

$$\tau = \sigma' \tan \varphi \qquad \text{Eq (1)}$$

$$\sigma' = \sigma - u \qquad \text{Eq (2)}$$

where

τ = shear strength
σ' = effective normal stress
σ = total normal stress
u = pore pressure
φ = angle of internal friction

When saturated loose sands are subjected to earthquake loading, primarily induced by upward propagation of shear waves from bedrock, they tend to settle and densify. However, the duration of the cyclic stress application is so short compared to the time required for water to drain, that the soil volume contraction cannot occur immediately and excess pore pressure will progressively build up. When the pore pressure equals the total stress, thereby reducing the effective stress to zero, sands will, at least temporarily, completely lose their stiffness and shear strength. Such a state is referred to as "initial liquefaction". At the onset of initial liquefaction, loose sands will undergo unlimited deformations or flow without mobilizing significant resistance to deformation. As a result, structures supported above or within the liquefied deposit undergo significant settlements and tilting; water flows upward to the surface creating sand boils; and buried pipelines and tanks may become buoyant and float to the surface. This phenomenon is referred to as "liquefaction" and is obviously a condition to be avoided in any type of major construction.

Relatively dense deposits of sand require more repetitions of cyclic stresses or cyclic stresses of greater intensity before they develop the state of initial liquefaction. However, subsequent seismic stress applications will lead to the pore pressure decrease caused by the tendency for dilation. The soil will, therefore, develop sufficient shear resistance to prevent further flow. During the process of developing the resistance, the soil will have to undergo some degree of deformation. As the seismic loading continues, the amount of deformation required to produce a stable condition may increase, but it never becomes larger than a certain limit. Various investigators have referred to this phenomenon as "initial liquefaction with limited strain potential", "cyclic mobility", or other similar terms.

In this report, liquefaction potential refers to any of the entire spectrum of events resulting from the application of seismic shear stresses to saturated cohesionless soil deposits that could ultimately give rise to a loss of shearing resistance or to the development of excessive strains.

1.4 Seismicity of the State of New York

The northeast United States (NEUS) lies within the relatively tectonically stable and geologically old North American plate, where a great deal of the tectonic action took place over two hundred million years ago when the Atlantic basin began to form due to the separation of Africa from North America. However, based on instrumental seismic records, earth scientists believe that the tectonic activity in the Northeast is still going on (Barosh, 1984; Ebel, 1987; Zoback, 1987) and that earthquakes with a magnitude equal to the October 17, 1989, Loma Prieta earthquake could also strike, but less frequently, any location in the NEUS. Such an occurrence would affect a much wider area and create more damage than in the western United States. This is because the Earth's

crust in the eastern states is probably harder, older and colder. It tends to transmit seismic energy more efficiently, at a very low rate of attenuation. According to Jacob (1991), for any given earthquake magnitude, the resulting ground shaking in the eastern US can reach distances 3 to 6 times further, thus affecting areas 10 to 40 times larger than in the western US. During the May 25, 1988 Saguenay earthquake of magnitude 6.0 in nearby Quebec, liquefaction was observed at a distance of 15 ½ miles (25 km) from the epicenter. This distance is approximately 10 times larger than the maximum distance of observed liquefaction in the western US during similar magnitude earthquakes (Law, 1990). Other features of the eastern US seismic hazards that differ from those in the western US are as follows (Jacob, 1992):

- Lack of surface faulting, i.e., potential loci of future quakes are not well known.
- Higher high-frequency content of seismic ground motions to large distance.
- Higher contrast of shaking on soft soils versus underlying hard rock, i.e., high site amplification.

New York State historically has been stricken by earthquakes with foci or hypocenters located not only within the State but also elsewhere in the eastern United States and Canada. For example, the 1811-1812 New Madrid earthquakes in Missouri and the 1988 Saguenay earthquake in Quebec were felt in Albany. Earthquake activity from 1534 to 1986 in the NEUS and adjacent areas is shown in Figure 1 (Ebel, 1987). Significant earthquakes that have occurred in New York State and Canada from 1737 to 1991 are listed in Table 1 (Earthquake Information Bulletin, 1975; Kulhawy and Ninyo, 1977; Mitronovas and Nottis, 1984; NCEER, 1990). Figure 2 (Mitronovas, 1982) shows a preliminary seismic zonation map of the State, in which four zones have been identified.

Zone A, covering the eastern and northern parts of the Adirondacks, is considered as the most seismically active area in the State. It is also part of a much larger active area trending NW-SE that extends into the St. Lawrence River Valley of Canada. The largest known earthquake in the State occurred in this zone on September 5, 1944, near Massena, St. Lawrence County. This event had a magnitude of 5.6 and caused over $16 million dollars in damage. The areas of greatest damage in this quake involved the sensitive Leda clay, in which earthquake shaking is believed to have led to large strength losses triggering landslides (Tuttle and Seeber, 1989).

Zone B can be considered as part of a larger active area extending south and southwest through New Jersey and into eastern Pennsylvania. Earthquake events in this zone are generally associated with geological structures such as the Ramapo Fault System, the 125th Street Fault and Dyckman Street Fault in upper Manhattan, the Dobbs Ferry Fault in Westchester County and some off-shore faults (Jacob, 1991). One of the earliest documented large earthquakes in Zone B occurred near Rockaway Beach in Queens County on August 10, 1884. This 5.0 magnitude event was felt throughout most of the NEUS and as far as Maryland. Some buildings tilted and settled into the sand on Coney Island and Long Island, possibly due to the liquefaction of beach deposits (Tuttle and Seeber, 1989). This quake caused only slight damage because much of Long Island was farm country then. It is believed that an earthquake of such magnitude, if striking today, could cause an estimated $2.0 billion dollars in damage on Mahattan Island and that an M=6.0 quake could cause over $11 billion dollars in damage.

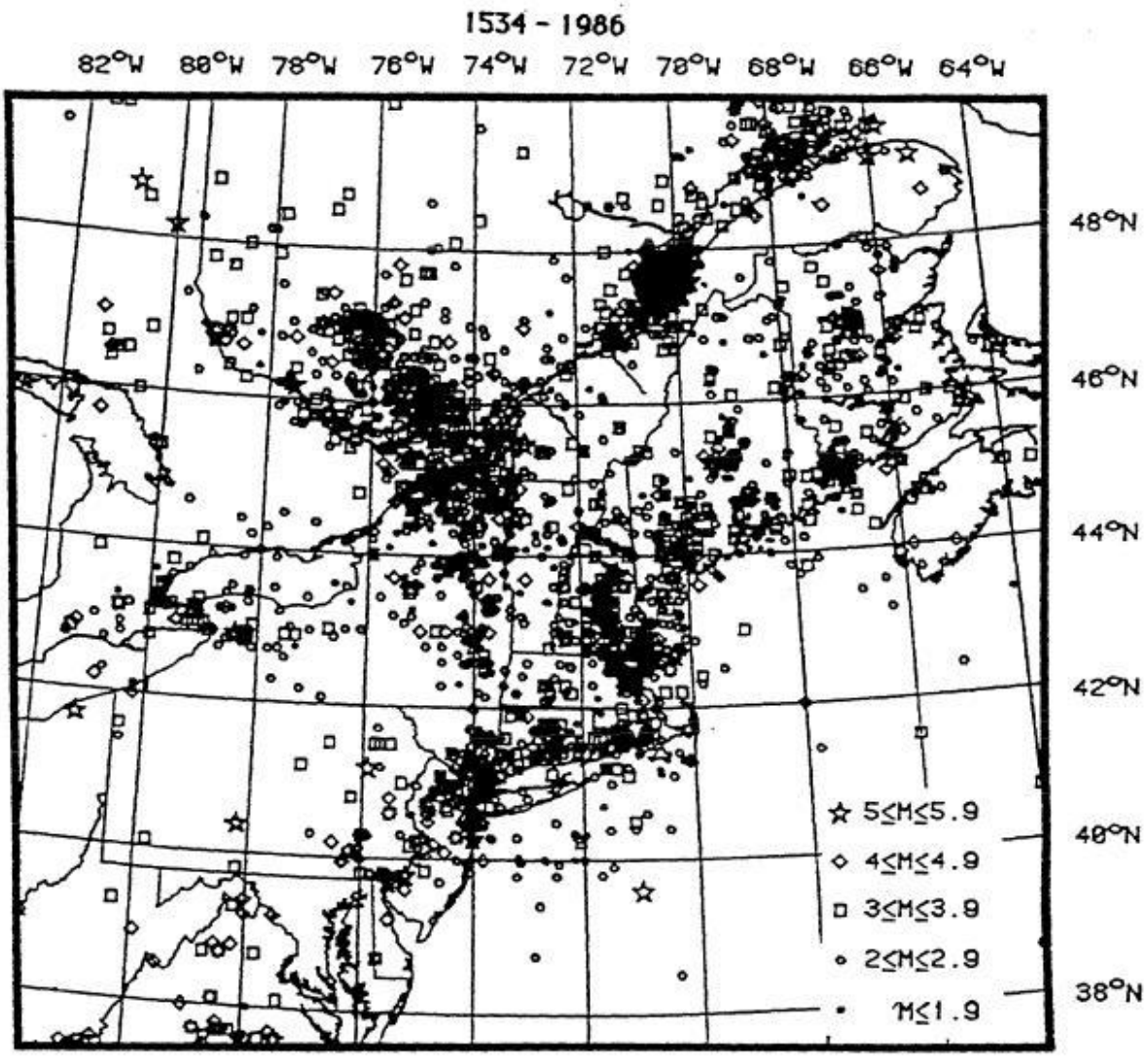

Figure 1 Map of all known earthquake activity from 1534 to 1986 for the northeast United States and adjacent Canada (Ebel, 1987)

Table 1

Significant Earthquakes in Northeast United States and Canada from 1534 to 1991

Date	Locality	Location		Modified Mercalli Intensity (MMI)	Magnitude M
		Latitude (North)	Longitude (West)		
1534 - 1535	St. Lawrence Valley			IX-X	
1638	St. Lawrence Valley			IX	
Feb. 5, 1663	Charlevoix, Quebec	47.6	70.1	X	7.0*
Nov. 9, 1727	Near Newburg, MA	42.8	70.8	VIII	7.0*
Dec. 19, 1737	Near New York City	40.60	73.80	VI	4.8
Nov. 18, 1755	Near Cape Ann, MA			VIII	6.2
Jan. 16, 1840	Herkimer	43.00	75.00	V-VI	
Mar. 12, 1853	Near Lowville	43.70	75.50	VI	4.8
Oct. 23, 1857	Near Buffalo	43.20	78.60	VI	
Oct. 17, 1860	Charlevoix, Quebec	47.50	70.10	VIII-IX	6.0*
Dec. 18, 1867	Canton	44.05	75.15	VI	4.8
Oct. 20, 1870	Charlevoix, Quebec	47.40	70.5	IX	6.5*
Dec. 11, 1874	Tarrytown	41.00	73.90	VI	4.8
Aug. 10, 1884	Rockaway Beach	40.59	73.84	VI	5.0
Mar. 8, 1893	Astoria	40.78	73.92	V-VI	
May 28, 1897	South of Plattsburgh	44.50	73.50	VI	
Feb. 3, 1916	Mohawk Valley	42.80	73.90	V-VI	
Feb. 28, 1925	Charlevoix, Quebec	47.60	70.10	IX	7.0*
Mar. 18, 1928	Saranac Lake	44.50	74.30	V-VI	4.1
Aug. 12, 1929	Attica	42.90	78.40	VII	5.2
Apr. 20, 1931	Lake George	43.50	73.80	VII	4.5
Apr. 15, 1934	Dannemora	44.70	73.80	V-VI	4.5
Nov. 1, 1935	Timiskaming, Quebec	46.50	79.00	VIII	6.0*
Sep. 5, 1944	Massena	45.00	74.70	VIII	5.6
Jan. 1, 1966	Attica - Varysburg	42.84	78.25	VI	4.6
Jun. 13, 1967	Attica - Alabama	42.84	78.23	VI	4.4
Jun. 9, 1975	Plattsburgh			VI	4.2
1982	Franklin, NH			VI	4.8
1982	Miramichi, New			V	5.7
	Brunswick				
Oct. 7, 1983	Goodnow	43.97	74.25	VI	5.2
Nov. 25, 1988	Saguenay, Quebec				6.0
Jun. 17, 1991	Summit				4.0

*: Moment Magnitude

References: Earthquake Information Bulletin (1975), Kulhway and Ninyo (1977), Mitronovas and Nottis (1984), NCEER (1990)

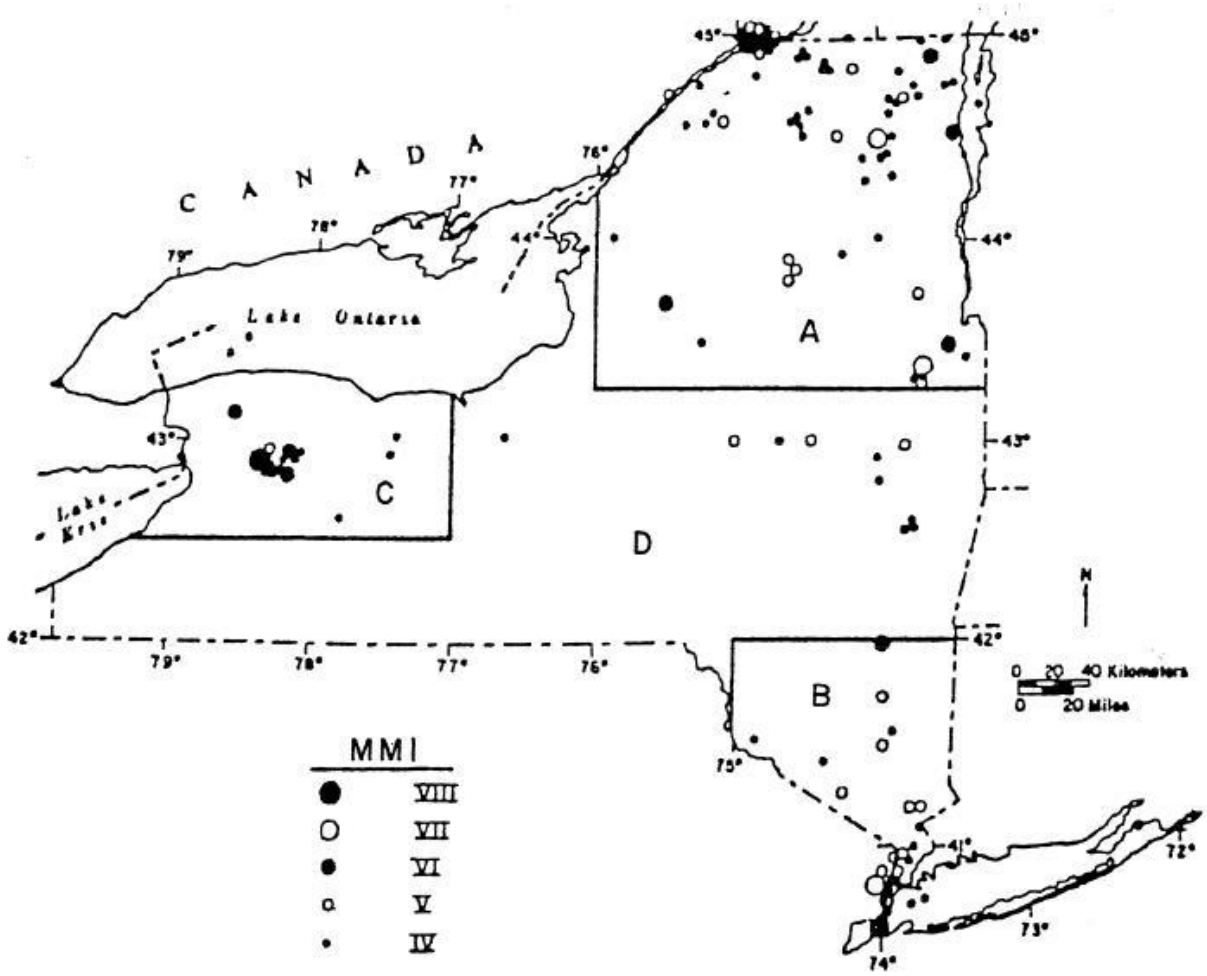

Figure 2 Seismic zonation map of New York (Mitronovas, 1982)

Zone C can be considered as another high risk seismic zone within the State, although the number of known earthquakes in this zone is smaller than that in Zones A and B. One of the largest earthquakes in the State occurred in this zone near Attica in Wyoming County on August 12, 1929. The area receiving the severest damage stretched from Southeastern Genesee County into north-central Wyoming County. The villages of Attica and Warsaw were significantly damaged. This event is believed to be associated with the Clarendon-Lindon Fault System, which may be the largest, oldest and most seismically active fault system in western New York.

Zone D, the central part of the State, has historically shown the least amount of seismic activity.

Fischer and McWhorter (1972) and Mitronovas (1982), based upon the available instrumental data, have suggested a possible north-south connection between Zones A and B along the eastern border of the State and that the mid-Hudson-Mohawk River valleys may be as seismically hazardous as Zone B.

According to the New York State Geological Survey (1989), earthquakes up to magnitudes of 6.0-6.5 are believed to be possible anywhere in the State. Earthquakes up to magnitudes of 7.0-7.5 are believed to be possible in Zones A and B. However, the state-of-the-art earthquake prediction technology is unable to predict when or where the next damaging earthquake in the State will occur, nor its severity.

1.5 Ground Motions

It is generally agreed, based upon analytical study and instrumental records, that earthquake magnitude, distance from the hypocenter and local subsurface conditions are the three major factors that affect the seismic intensity at the site. The larger the magnitude or shorter the distance from the earthquake focus, the stronger is the seismic intensity at a given site. In addition, the level of shaking intensity in rock is generally different from that in a soil deposit at ground surface or at any depth below the ground surface. Other factors being equal, local subsurface conditions alone can both amplify and attenuate earthquake forces. During small earthquakes and microtremors, the ground surface accelerations on soil deposits, especially on soft compressible clay layers and alluvial deposits, are usually higher than those occurring on bedrock. However, as earthquake magnitudes become greater, the horizontal accelerations on soil sites may be equal to or lower than those on rock sites.

Ground response due to soil amplification and soil attenuation is a complex subject and is beyond the scope of this report. However, the degree of amplification and attenuation of horizontal acceleration at the ground surface is believed to depend on factors (Dobry and Vucetic, 1987; Law, 1990) such as: soil type, consistency and natural period of the soil deposit, degree of stress-strain nonlinearity of the soil under shaking, dynamic soil properties, range of shear strains induced in the soil by earthquake, soil-structure interaction, local geological features, frequency content of the ground motions, etc. As noted by Ishihara (1985), when a soil layer is liquefied, the energy of the vertically propagating shear waves will, to a certain degree, be absorbed by the liquefied soil. As a result, the transmission of incoming acceleration to ground surface is depressed and the shaking intensity attenuated. He suggests using 0.2g as the maximum ground surface acceleration on top of a liquefied layer.

The rock acceleration coefficients, expressed as percent of gravity, for the State may be determined from the contour maps of Figures 3 and 4 (FEMA, 1988). The coefficients were mapped by the U.S. Geological Survey (Algermissen et al., 1982; 1990) at two different probability levels - 10 percent chance of exceedance in 50 and 250 years - to show relative hazard which may be appropriate for ordinary bridges and bridges providing critical services, respectively. Linear interpolation should be used for sites located between contour lines or between a contour line and a local maximum or minimum.

The maximum ground acceleration caused by an earthquake may be obtained from field measurements or numerical methods using the wave propagation theory (Idriss and Seed, 1968; Schnabel et al., 1972; Finn et al., 1976; Liou et al., 1977; Martin and Seed, 1978; Singh et al., 1981; Prevost, 1989). The most widely used numerical method to estimate the ground site response has been a quasi-linear total stress analysis using the computer program SHAKE developed by Schnabel et al. (1972), in which nonlinear stress-strain behavior of soil is accounted for by adjusting shear modulus and damping, iteratively, until the computed dynamic shear strains converge. For design simplicity, Seed et al. (1976) established approximate relationships between maximum accelerations on rock and maximum ground accelerations for various subsurface conditions, as shown in Figure 5. It shows that maximum horizontal accelerations on rock and on stiff soil sites are almost identical over a wide range of accelerations. The curve that represents soft to medium clay and sand sites is believed to be unconservative for soft and medium clays in estimating the maximum ground accelerations and, therefore, should not be used for such soil deposits for any design purposes. Idriss (1990) modified this curve to Figure 6 based on the ground motion data obtained at soft clay sites in the 1985 Mexico City earthquake and the 1989 Loma Prieta earthquake and a number of site response analyses of soft clay deposits subjected to the 1964 Alaska acceleration time history. This figure indicates that bedrock accelerations beneath soft soil sites are generally amplified by the soft sediment below 0.4g and attenuated above 0.4g.

Figure 3 Map of horizontal accelerations (expressed as percent of gravity) in rock with 10% probability of being exceeded in 50 years (Algermissen et al., 1982; 1990)

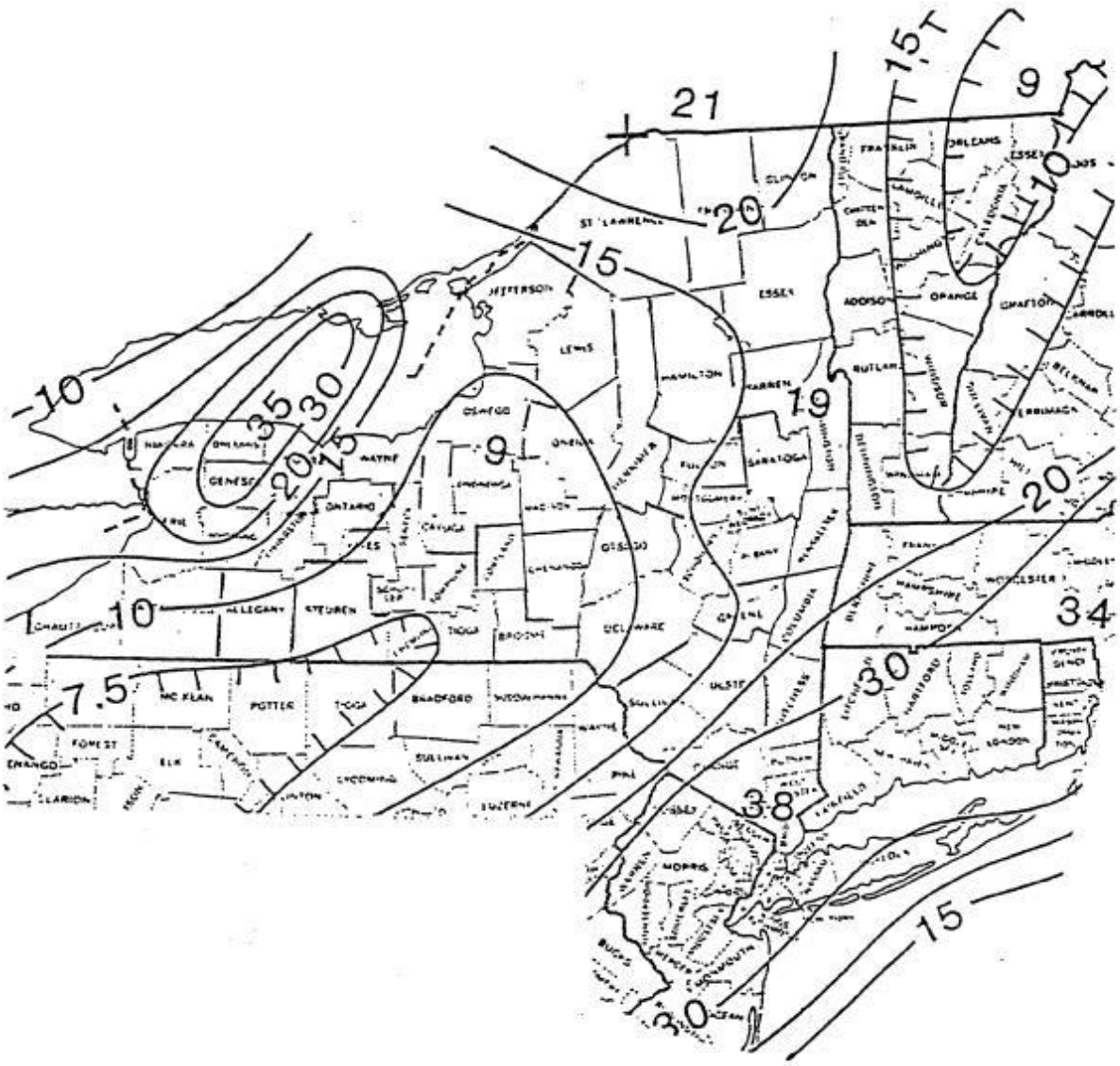

Figure 4 Map of horizontal accelerations (expressed as percent of gravity) in rock with 10% probability of being exceeded in 250 years (Algermissen et al., 1982; 1990)

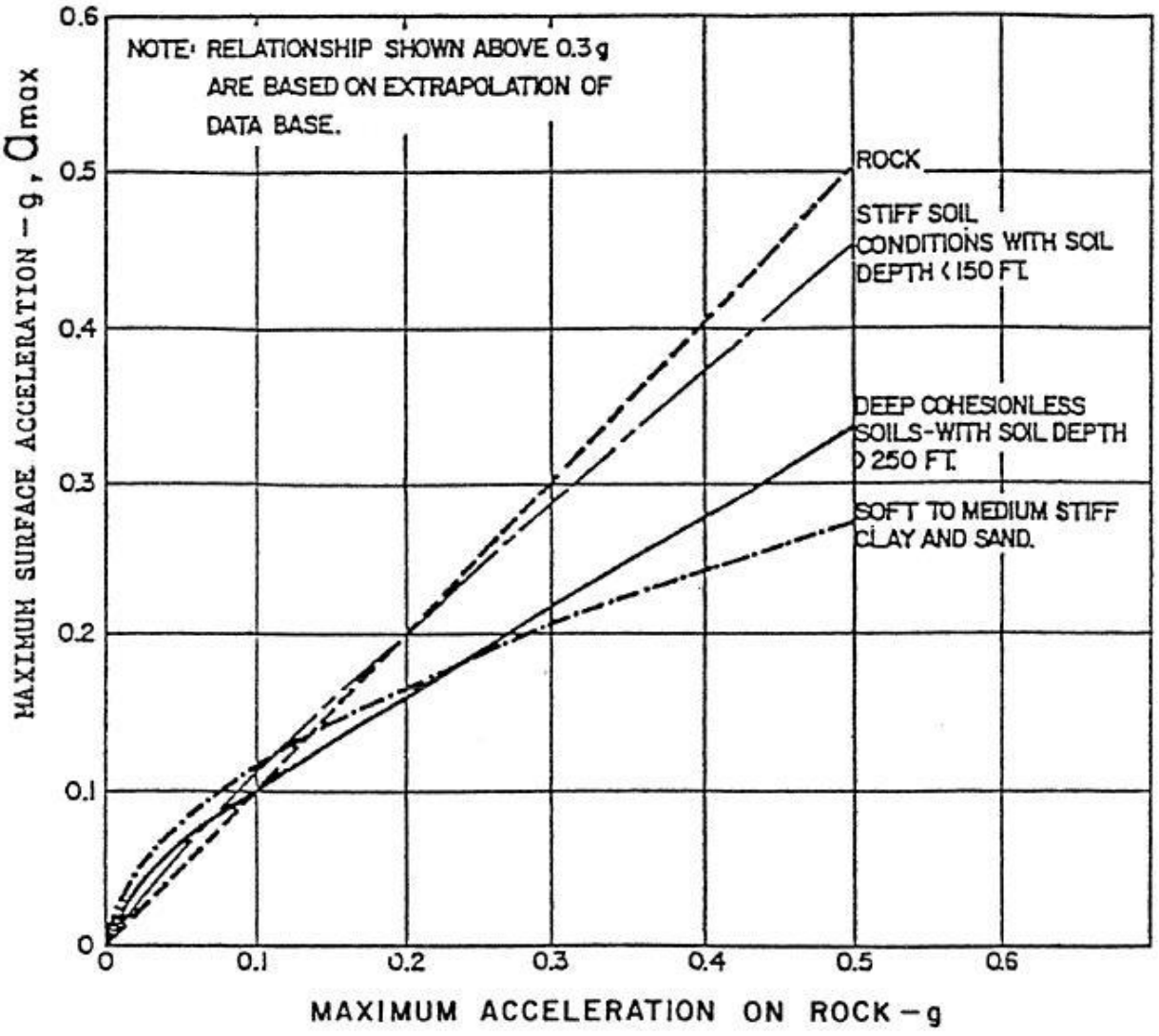

Figure 5 Approximate relationship between maximum accelerations on rock and maximum ground accelerations (Seed et al., 1976)

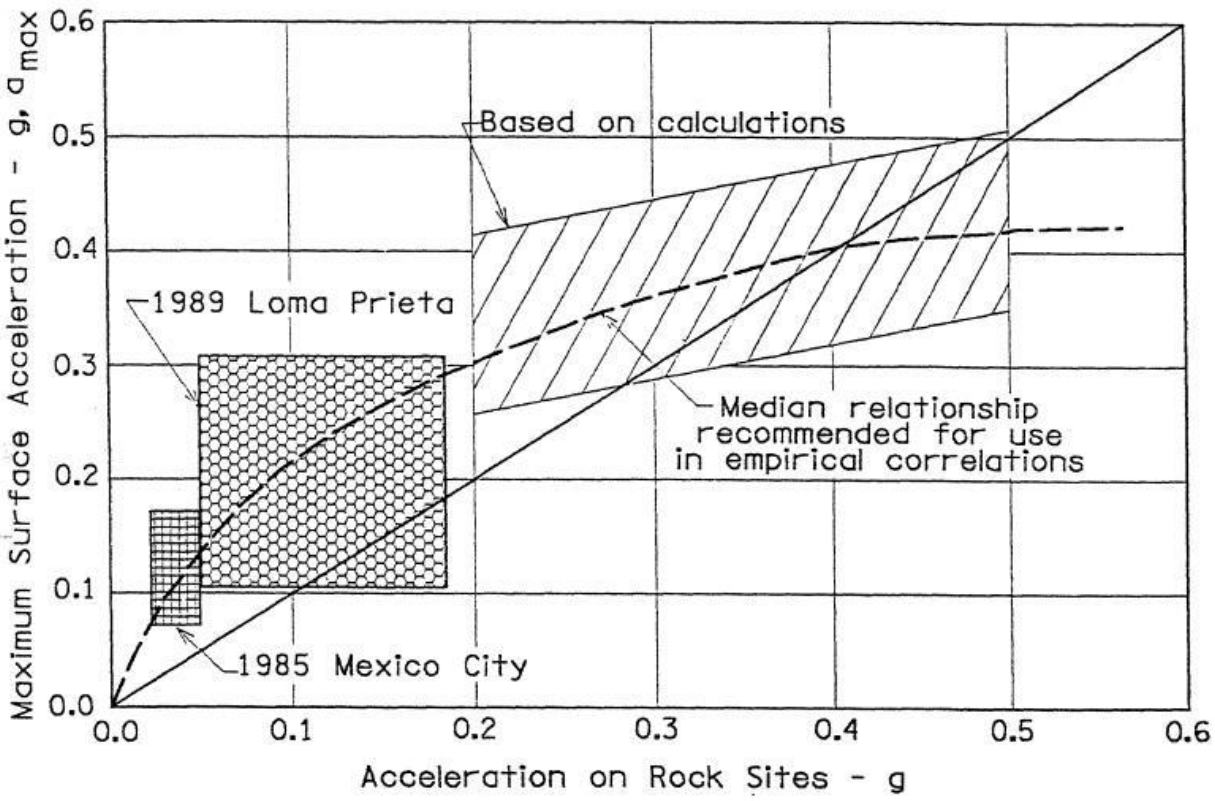

Figure 6 Amplification – attenuation relationship for modifying bedrock acceleration at soft soil sites (Idriss, 1990)

However, special precautions should be taken when using this curve because it represents the ground response of a number of soft, sensitive and highly plastic clay deposits, which tend to have relatively lower damping values under seismic loading than those of low to medium plasticity clays. For ordinary bridges founded on deposits of stiff soils and cohesionless soils, the maximum ground accelerations obtained from Figures 3 and 5 may be used to evaluate the liquefaction potential of the foundation soils (see Section 3.2). However, for projects involving soft soils and for bridges providing critical services, a special site-specific seismic response study may be required to determine the design maximum ground acceleration.

2. FAILURE TYPES AND FACTORS AFFECTING LIQUEFACTION SUSCEPTIBILITY

2.1 Failure Types

There are four basic types of ground failure that commonly result from liquefaction: flow failure, lateral spread, ground oscillation and loss of bearing capacity. Other phenomena associated with liquefaction include rise of pore water pressure, sand boils and various types of deformation. Sand boils, by themselves, are not strictly a form of ground failure, but rather are diagnostic evidence of pore water pressure buildup at depth, indicating that liquefaction has occurred.

2.1.1 Flow Failures

Flow failures occur in sloping areas inclined at 5 percent or greater and are basically landslides on a very large scale. They are the most damaging type of ground failure caused by liquefaction. Flow failures occur when a mass of loose granular soil loses its strength after initial liquefaction and flows like a heavy liquid producing very large deformations. The incipient condition for the inducement of flow type deformation is closely associated with the residual strength or steady-state strength which is mobilized in soils after they have undergone deformations. Flow failures commonly displace large masses of soil for hundreds of feet (meters).

Materials involved in flows may consist of completely liquefied soil or blocks of intact material riding on a layer of liquefied soil. Flow failures may occur in natural ground, but are also likely in man-made earth structures, such as earth dams, mine-tailing dams and fill placed behind waterfront retaining structures. The earliest known flow failures in the U.S. occurred in the 1811-1812 New Madrid earthquake in Missouri (Fuller, 1912). More recently, the failure of the upstream slope of the Lower San Fernando Dam during the 1971 San Fernando, California, earthquake is another notable example of flow failure (Seed et al., 1975).

2.1.2 Lateral Spreading

Lateral spreading is the most common type of ground failure triggered by liquefaction (Varnes, 1978). Primarily, it involves lateral displacement of large, blocks of intact, surficial soil as a result of liquefaction in underlying layers (see Figure 7). Other phenomena such as rotational movements and subsidence occur during lateral spreading. Lateral spreads generally develop on gentle slopes, as flat as 3 degrees, and move toward a free face, such as an incised river channel. Permanent displacements ranging from a few inches (centimeters) to over 30 ft. (10 m) have been observed in the U.S., Japan and other countries, causing damage to embankments, buried pipelines, roads, bridges, foundations of buildings and canals (National Research Council, 1985; Youd and Perkins, 1987). During the 1964 Alaska earthquake, for example, 266 bridges were displaced and damaged by spreading of flood plain deposits toward river channels. All of these bridges were supported on piles and in nearly all instances the tops were laterally displaced.

In their 1992 review of several hundred case histories that involve earth failures from earthquakes, Barlett and Youd found that the potential for significant lateral displacement due to liquefaction diminishes tremendously for earthquake magnitudes below 6 and that no significant lateral spreading is likely to occur in dense to very dense sands if the magnitude of

the earthquake is less than 8.

2.1.3 Ground Oscillation

When the ground is too flat to permit lateral movement, liquefaction at depth may create separations at the surface by decoupling overlying soil blocks, allowing the blocks to jostle back and forth on the liquefied layer, as shown in Figure 8. This phenomenon of soil block jostling produces an oscillation as ground waves. It is reported (Youd, 1984) that the decoupled surface layer vibrates in a different mode than the underlying and surrounding firm ground, causing fissures to form and impacts to occur between oscillating blocks and adjacent firm ground.

Ground oscillation and associated sand boils can present an enormous clean-up problem if they occur in a built-up area. If accompanied by ground settlement, damage and disruption can also occur.

2.1.4 Loss of Bearing Capacity

When the soil supporting a structure liquefies and loses strength, large deformations can occur, leading to large settlements and/or tilting of structures. Loss of soil bearing capacity may also occur when liquefaction that has initially developed in a sand layer a few meters below a footing propagates upward through overlying sand layers and subsequently weakens the soil supporting the structure.

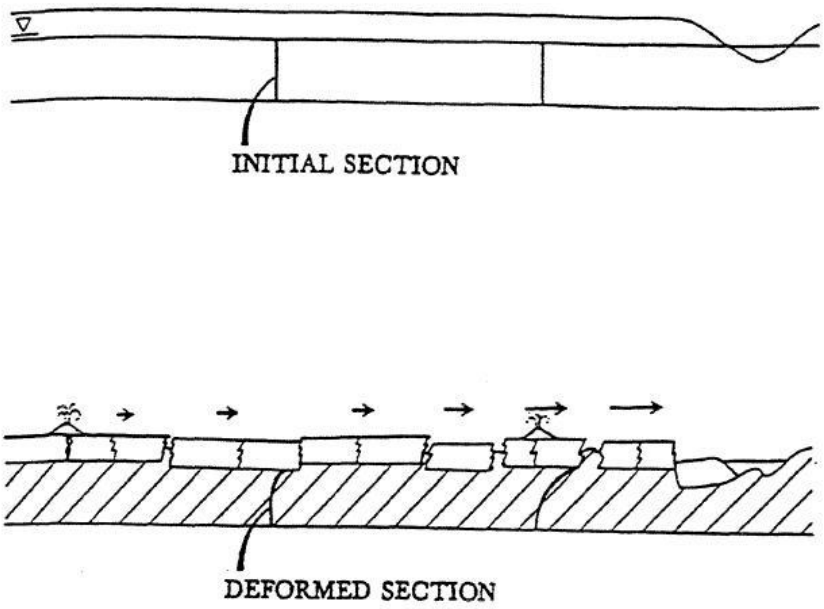

Figure 7 Lateral spread before and after liquefaction (Youd, 1984)

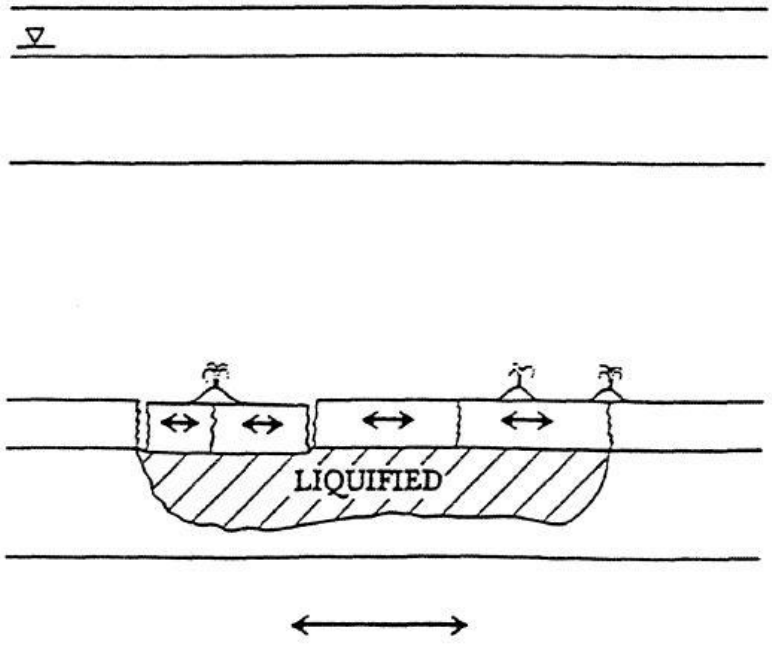

Figure 8 Ground oscillation before and after liquefaction (Youd, 1984)

Table 2 contains a list of structures sensitive to liquefaction and the type of instability to which each structure is most vulnerable.

TABLE 2
Classes of Liquefaction-Induced Structural Instability (National Research Council, 1985)

Structures Most Often Affected	Types of Structural Instability
Buried and surface structures	Loss of foundation bearing capacity
Structures built on or at the base of a slope	Slope instability slides
Dam embankments and foundations	Slope instability slides
Bridge piers Railway lines Highways Utility lines	Movement of liquefied soil adjacent to topographic depressions
Structures, especially those with slabs on grade Utility lines Highways Railways	Lateral spreading on horizontal ground
Buried tanks Utility poles	Excess structural buoyancy caused by high subsurface pore pressure
Structures built on grade	Formation of sink holes from sand blows
Retaining walls Port structures	Increase of lateral stress in liquefied soil

2.1.5 Effects of Liquefaction on Piles

During a seismic event, the dynamic response of piles will be affected by the nature of the earthquake loading, the pile and soil characteristics, and the degree of restraint applied by the superstructure to the motion of the pile. If the soil deposits at the structure site are liquefied, the pile-supported structure may be damaged or destroyed by mechanisms associated with different types of ground failure as stated in Sections 2.1.1 - 2.1.4. To improve the pile performance during an earthquake, the following effects of liquefaction on piles should be considered in the foundation design:

1. Decrease or loss in vertical pile load capacity from both skin and end bearing resistances, depending upon the zone of liquefaction along the pile depth.
2. Decrease in lateral pile load capacity and increase in lateral deflection: Especially if the liquefaction occurs near the surface and extends only to a limited portion of the total pile depth.
3. Increase in pile settlement: Any decrease in skin or end bearing resistance may result in some pile settlement. However, if the soil below an end bearing pile liquefies, objectional settlement and possible damage to the structure may also occur.
4. Increase in pile load from downdrag forces caused by the settlements of the liquefied or partially liquefied soils along the pile length.

2.2 Factors Affecting Liquefaction Susceptibility

Based on field observation and laboratory testing results, liquefaction characteristics of cohesionless soils are affected by a number of factors:

2.2.1 Grain-Size Distribution and Soil Types

The type of soil most susceptible to liquefaction is one in which the resistance to deformation is mobilized by friction between particles. If other factors such as grain shape, uniformity coefficient and relative density are equal, the frictional resistance of cohesionless soil decreases as the grain size of soils becomes smaller. Tsuchida (1970) summarized the results of sieve analyses performed on a number of alluvial and diluvial soils that were known to have liquefied or not to have liquefied during earthquakes. He proposed ranges of grain size curves separating liquefiable and nonliquefiable soils as shown in Figure 9. The area within the two inner curves in the figure represents sands and silty sands, the soils with the lowest resistance to liquefaction. A soil with a gradation curve falling in the zones between the outer and inner curves is less likely to liquefy. Soils with a higher percentage of gravels tend to mobilize higher strength during shearing, and to dissipate excess pore pressures more rapidly than sands. However, there are case histories indicating that liquefaction has occurred in loose gravelly soils (Seed, 1968; Ishihara, 1985; Andrus, et al., 1991) during severe ground shaking or when the gravel layer is confined by an impervious layer. The space between the two curves farthest to the left reflects the influence of fines in decreasing the tendency of sands to densify during seismic shearing. Fines with cohesion and cementation tend to make sand particles more difficult to liquefy or to seek denser arrangements. However, nonplastic fines such as rock flour, silt and tailing slimes may not have as much of this restraining effect. Ishihara (1985) stated that clay- or silt-size materials having a low plasticity index value will exhibit physical characteristics resembling those of cohesionless soils, and thus have a high degree of potential for liquefaction. Walker and Steward (1989), based on their extensive dynamic tests on silts, have also concluded that nonplastic and low plasticity silts, despite having their grain size distribution curves outside of Tsuchida's boundaries for soils susceptible to liquefaction, have a potential for liquefaction similar to that of sands and that increased plasticity will reduce the level of pore pressure response in silts. This reduction, however, is not significant enough to resist liquefaction for soils with plasticity indices of 5 or less.

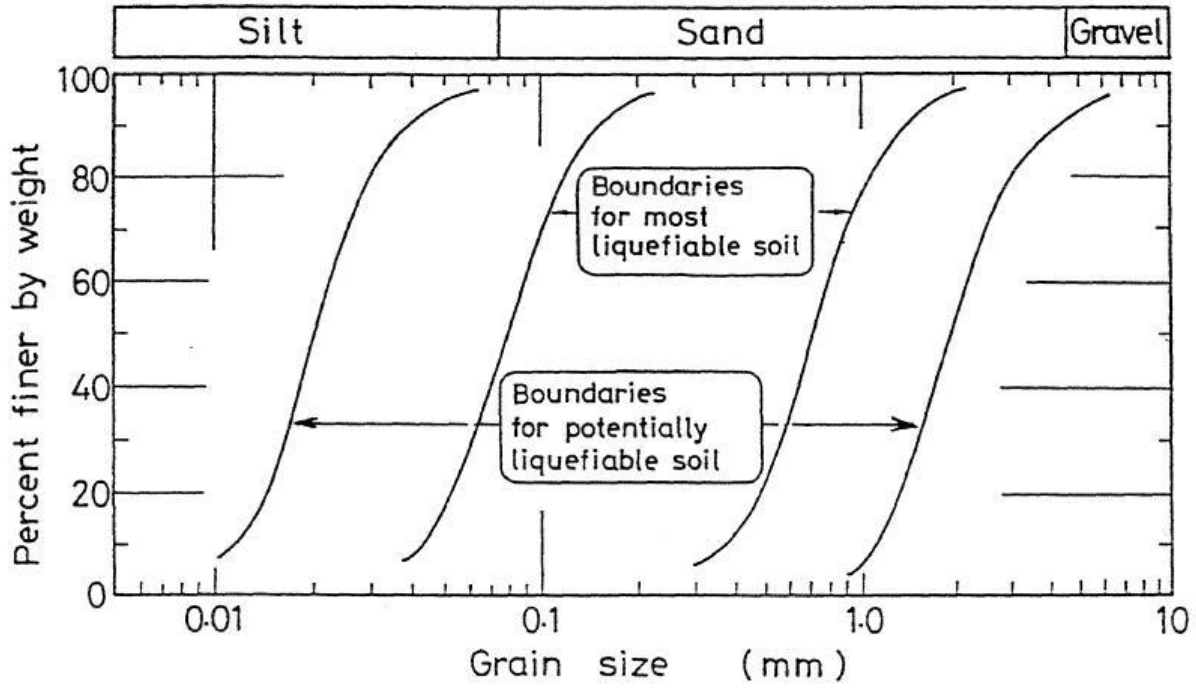

Figure 9 Limits in the gradation curves separating liquefiable and nonliquefiable soils (Tsuchida, 1970)

Even though major slide movements during earthquakes have occurred in clay deposits, they are commonly considered to be nonliquefiable during earthquakes in the sense that an extensive zone of clay soil is converted into a heavy fluid condition. However, it is believed that quick clays may lose most of their strength after strong shaking and that other types of clay may lose a proportion of their strength resulting in slope failures. Frequently, landslides in clay deposits containing sand or silt lenses are initially triggered by the liquefaction of these lenses before any significant strength loss occurs in the clay. This has been supported by laboratory test results which indicate that the strain required to liquefy sands is considerably smaller than the strain required to overcome the peak strength of cohesive soils (Seed, 1968; Poulos, Robinsky and Keller, 1985).

There is also ample evidence to show that uniformly graded materials, generally having a uniformity coefficient smaller than five, are more susceptible to liquefaction than well-graded materials (Ross, et al., 1969; Lee and Fitton, 1969) and that for uniformly graded soils, fine sands tend to liquefy more easily than coarse sands, gravelly soils, silts or clay.

2.2.2 Relative Density

Laboratory test results and field case histories indicate that, for a given soil, initial void ratio or relative density is one of the most important factors controlling liquefaction. Liquefaction occurs principally in saturated clean sands and silty sands having a relative density less than 50%. For dense sands, however, their tendency to dilate during cyclic shearing will generate negative pore water pressures and increase their resistance to shear stress. The lower limit of relative density beyond which liquefaction will not occur is about 75%.

2.2.3 Earthquake Loading Characteristics

The vulnerability of any cohesionless soil to liquefaction during an earthquake depends on the magnitude and number of cycles of stresses or strains induced in it by the earthquake shaking. These in turn are related to the intensity, predominant frequency, and duration of ground shaking.

2.2.4 Vertical Effective Stress and Overconsolidation

It is well known that an increase in the effective vertical stress increases the bearing capacity and shear strength of soil, and thereby increases the shear stress required to cause liquefaction and decreases the potential for liquefaction. From field observations it has been concluded by a number of investigators that saturated sands located deeper than 50 to 60 feet (15 to 18 m) are not likely to liquefy. These depths are in general agreement with Kishida (1969) who states that a saturated sandy soil is not liquefiable if the value of the effective overburden pressure exceeds 2 tsf (190 kN/m^2).

Both theory and experimental data show that for a given soil a higher overconsolidation ratio leads to higher lateral earth pressure at rest and thereby increases the shear stress ratio required to cause liquefaction.

2.2.5 Age and Origin of the Soils

Natural deposits of alluvial and fluvial origins generally have soil grains in the state of loose packing. These deposits are young, weak and free from added strength due to cementation and

aging. Youd and Hoose (1977) stated that, as a rule of thumb, alluvial deposits older than late Pleistocene (10,000- 130,000 years) are unlikely to liquify except under severe earthquake loading conditions, while late Holocene deposits (1,000 years or less) are most likely to liquefy, and earlier Holocene (1,000-10,000 years) deposits are moderately liquefiable.

2.2.6 Seismic Strain History

It has been demonstrated from laboratory test results that prior seismic strain history can significantly affect the resistance of soils to liquefaction (Finn et al., 1970; Seed et al., 1977; Singh et al., 1980). Low levels of prior seismic strain history, as a result of a series of previous shakings producing low levels of excess pore pressure, can significantly increase soil resistance to pore pressure buildup during subsequent cyclic loading. This increased resistance may result from uniform densification of the soil or from better interlocking of the particles in the original structure due to elimination of small local instabilities at the contact points without any general structural rearrangement taking place. Large strains, however, associated with large pore pressure generation and conditions of full liquefaction can develop weak zones in the soil due to uneven densification and redistribution of water content (National Research Council, 1985; Whitman, 1985), and thus lower the resistance of the soil to pore pressure generation during subsequent cyclic loading.

2.2.7 Degree of Saturation

Liquefaction will not occur in dry soils. Only settlement, as a result of densification during shaking, may be of some concern. Very little is known on the liquefaction potential of partially saturated sands. Available laboratory test results (Sherif et al., 1977) show liquefaction resistance for soils increases with decreasing degree of saturation, and that sand samples with low degree of saturation can become liquefied only under severe and long duration of earthquake shaking.

2.2.8 Thickness of Sand Layer

In order to induce extensive damage at level ground surface from liquefaction, the liquefied soil layer must be thick enough so that the resulting uplift pressure and amount of water expelled from the liquefied layer can result in ground rupture such as sand boiling and fissuring (Ishihara, 1985; Dobry, 1989). If the liquefied sand layer is thin and buried within a soil profile, the presence of a nonliquefiable surface layer may prevent the effects of the at-depth liquefaction from reaching the surface. Ishihara (1985) has set up a criterion to stipulate a threshold value for the thickness of a nonliquefiable surface layer to avoid ground damage due to liquefaction, as shown in Figure 10. Although this figure is believed to be speculative and should not be used for design purposes, it provides initial guidance in this matter for sites having a buried liquefiable sand layer with a standard penetration resistance of less than 10 blows per foot (0.3 m). It should also be noted that even though the thickness of a nonliquefiable surface layer exceeds the threshold thickness shown in the figure, the ground surface may still experience some settlement which may be undesirable for certain settlement-sensitive structures. Like all of the empirical curves shown in this report, this figure, based on just three case histories, may need to be modified as more data become available.

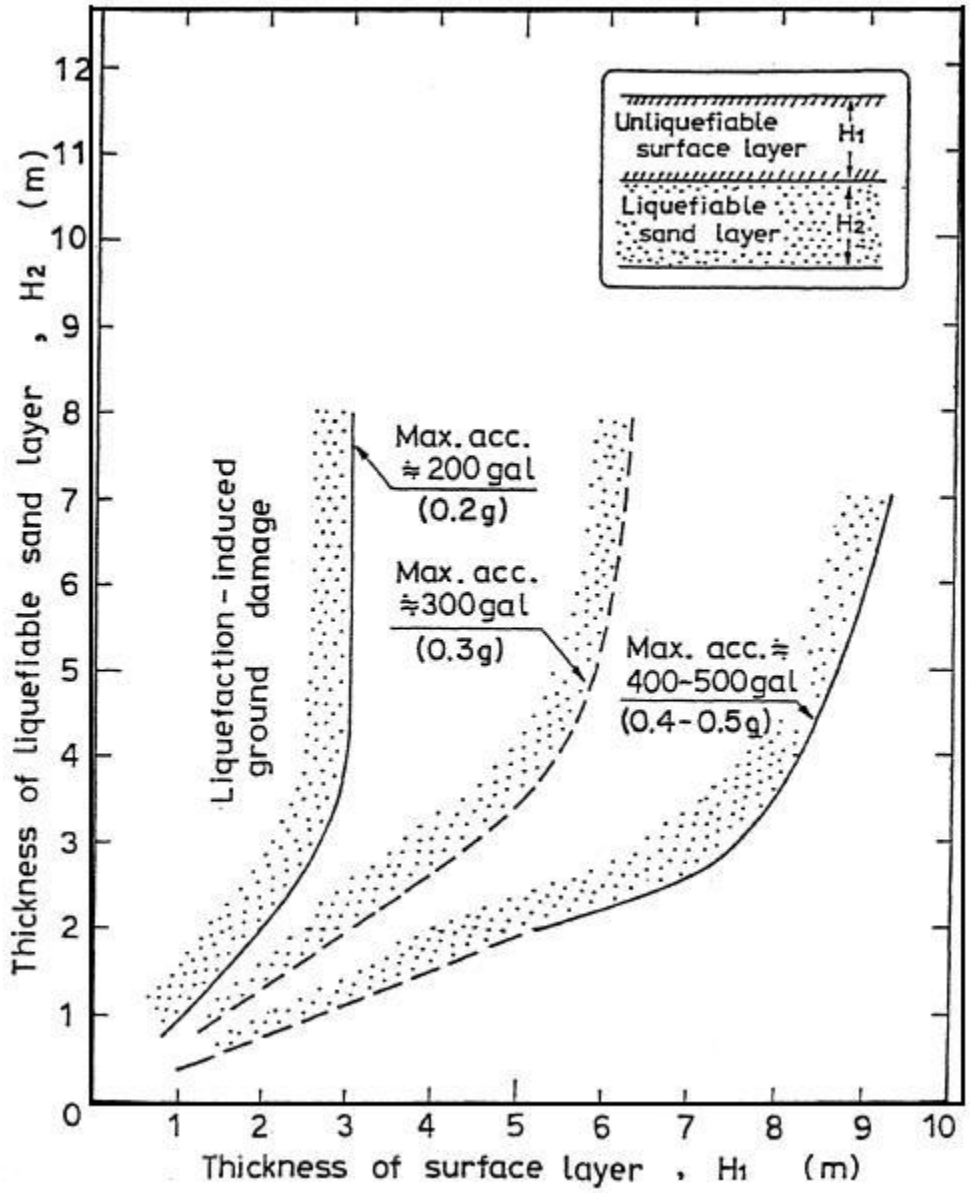

Figure 10 Proposed boundary curves for site identification of liquefaction-induced damage (Ishirhara, 1985)

3. EVALUATION OF LIQUEFACTION POTENTIAL

3.1 Introduction

Various procedures for evaluating the liquefaction potential of saturated soil deposits have been proposed in the past twenty years. These procedures, requiring various degrees of laboratory and/or in-situ testing, may be classified into the following categories:

1. **Mapping Based on Geological Criteria:**
   A method for constructing liquefaction potential maps was developed by Youd and Perkins (1978), relating geological age, origin of sediments and site distance to the potential earthquake epicenter. The proposed criteria are widely used for general assessment of regional liquefaction hazards (Youd et al., 1978; Anderson et al., 1982; Tinsley et al., 1985).

2. **Empirical Correlations Between In-Situ Characteristics and Observed Performance**
   Soil liquefaction characteristics determined by field performance have been correlated with a variety of soil parameters such as
   a. Standard Penetration Test (SPT) Resistance (Seed and Idriss, 1971; Seed, 1979; Seed et al., 1983, 1985; Ishihara, 1985)
   b. Cone Penetration Resistance (Douglas et al., 1981; Robertson et al., 1983; Kovas et al., 1984; Baldi et al., 1985; Robertson and Campanella, 1985; Seed et al., 1985;)
   c. Shear Wave Velocity (Dobry et al., 1981; Campanella and Robertson, 1984; Bierschwale and Stokoe, 1984)
   d. Resistivity and Capacitance of Soil (Arulanandan, 1977; Arulmoli et al., 1985)

3. **Threshold Shear Strain Concept**
   There exists for a given cohesionless soil a threshold shear strain, typically 0.01 percent. If the peak shear strain induced by an earthquake does not exceed this strain, the shaking will not cause a buildup of excess pore pressure regardless of the number of loading cycles, and, therefore, liquefaction cannot occur (Dobry et al., 1980). The peak shear strain caused by an earthquake ground motion may be estimated with reasonable accuracy using the following equation:

   $$r = 1.2\ a\ Z / Vs^2 \qquad \text{Eq (3)}$$

   where r equals strain, a equals peak acceleration at ground surface, Z equals depth, and Vs equals shear wave velocity.

4. **Liquefaction Probability**
   Probabilistic approaches to liquefaction analyses have been proposed by several researchers (Yegian and Whitman, 1978; Haldar and Tang, 1979; Fardis and Veneziano, 1982; Chameau and Clough, 1983; Liao et al., 1988). However, the usefulness of this approach depends on the soundness of the assumed mechanistic models and on the feasibility of quantifying uncertainty for model parameters.

5. **Steady-State Strength Concept for Analyzing Stability of Embankments and Slopes Against Flow Failures**
   The steady-state strength concept, founded on Casagrande's "Critical Void Ratio Theory"

(Casagrande, 1936), has been developed to evaluate the susceptibility of an embankment or slope to a liquefaction flow failure (Castro, 1969; Poulos, 1981; Castro et al., 1982; Poulos, Castro and France, 1985). Castro and Poulos have shown that even after liquefaction, many sands retain a strength which may be appreciable. Seed and his co-workers use the term residual strength to refer to the strength of liquefied materials. In this report, the terms steady-state and residual strengths are used interchangeably.

If the sand beneath an embankment or slope is very loose and has the type of stress-strain behavior shown in Figure 11, a seismic loading of sufficient intensity and duration can strain the soil over the peak of the stress-strain curve and trigger initial liquefaction. Once this condition is reached, creep and progressive failure will cause the shear resistance of the soil to continuously decline until the steady state or residual strength is reached. If the undrained steady-state strength is smaller than the initial shear stress required for static equilibrium, the slope will be destabilized and a flow failure will occur. Therefore, when a flow failure occurs, the reduced strength need not be zero, and, conversely, even a very low reduced strength may not lead to a flow failure if other soils along the potential failure surface are strong enough to prevent a loss of stability.

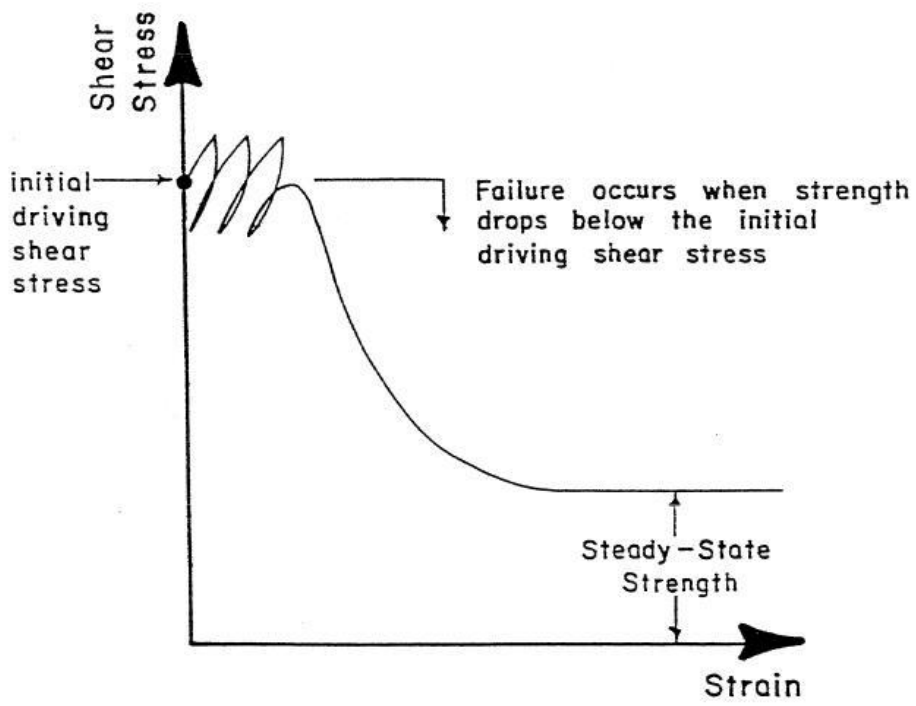

Figure 11 Undrained stress-strain curve for loose sand (Seed et al., 1989)

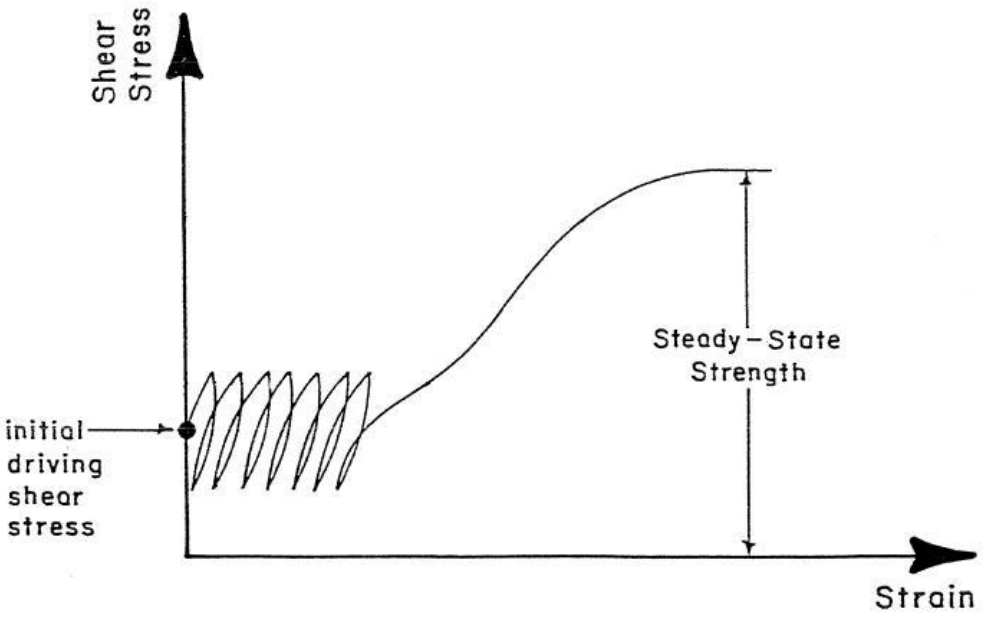

Figure 12 Undrained stress-strain curve for dense sand (National Research Council, 1985)

During earthquake shaking, dense sands have a tendency to dilate and generate negative pore water pressure. As a result, soil shearing resistance increases until a maximum value is reached, as shown in Figure 12. At the end of the shaking, the initial static shear stress is still less than the peak shear resistance. Therefore, slope instability is unlikely to occur in dense sands under earthquake loading.

The evaluation procedure involves laboratory steady-state strength testing followed by appropriate conservative corrections to the in-situ void ratio condition taking all relevant factors into account.

Of all the available methods described above, only two procedures will be summarized in separate sections below. They are (1) the empirical correlation based on the SPT blow count and field performance, and (2) a simplified steady-state procedure for analyzing stability of embankments and slopes against flow failures. These approaches have proved to give the most plausible results and will be considered by the Bureau as the only acceptable procedures for evaluating the liquefaction potential of cohesionless soils.

3.2 Evaluation of Liquefaction Potential of Horizontal Ground Using SPT Resistance

3.2.1 Sands and Silty Sands

Investigations based upon in-depth theoretical study and extensive review of field performance of sands and silty sands during actual earthquakes in the western United States, Alaska, South America, Japan and China, show that a high correlation exists between soil liquefaction resistance under earthquake shaking and soil SPT resistance in level ground conditions (Seed et al., 1983, 1985; Tokimatsu and Yoshimi, 1983). Based on this correlation, a design procedure for evaluating the liquefaction potential of level ground has been developed for the Bureau as follows:

a. Establish the soil profiles and identify the potentially liquefiable layers by comparing soil gradation curves with Figure 9. For projects involving only ordinary bridges, use a design earthquake magnitude of 6.00 for sites located in Zones A, B or C of Figure 2. A magnitude of 5.25 is used elsewhere in the State. However, a special seismic study may be required to determine the design earthquake magnitude for bridges providing critical services.

b. Compute the average induced cyclic shear stress ratio due to earthquake shaking for each potentially liquefiable layer using the following relationship (Seed and Idriss, 1971):

$$\tau_{av} / \sigma_o' = 0.65 \cdot (a_{max} / g) \cdot (\sigma_o / \sigma_o') \cdot Y_d \qquad \text{Eq (4)}$$

Where τ_{av} / σ_o' = earthquake-induced cyclic shear stress ratio

τ_{av} = average peak shear stress

a_{max} = maximum horizontal ground acceleration

σ_o = total overburden pressure at depth under consideration

σ_o' = effective overburden pressure at depth under consideration

Y_d = a stress reduction factor which decreases linearly from a value of 1 at the ground surface to a value of 0.9 at a depth of 35 ft. (10.67 m), use Figure 13 for depths greater than 35 ft. (10.67 m)

g = acceleration due to gravity

For ordinary bridges founded on deposits of cohesionless soils and stiff soils, choose a maximum ground acceleration from Figures 3 and 5. However, for projects involving soft soils and for bridges providing critical services, a special seismic site response study may be required to determine the design maximum ground acceleration.

c. Correct the measured New York State penetration resistance value, N_{NY}, to $(N_1)_{60}$ using the following formula:

$$(N_1)_{60} = 1.29\ C_N\ ER_m\ N_{NY}/60 \qquad \text{Eq (5)}$$

Where $(N_1)_{60}$= normalized standard penetration resistance under an effective overburden pressure of 1 tsf (95.76 kN/m^2) for an SPT test performed with a hammer providing 60% of the theoretical free-fall energy, in accordance with the conditions listed in Table 3

C_N = an overburden correction factor, equal to $(\sigma_o'/2000)^{-1/2}$ but not greater than 2.0, where σ_o' is in psf, or $(\sigma_o'/95.76)^{-1/2}$ where σ_o' is in kN/m^2 (Liao and Whitman, 1985)

ER_m = energy ratio defined as the percent of theoretical free fall energy delivered to the drill rods. A summary of the average energy ratios used in different countries using different types of hammers and hammer release mechanisms is shown in Table 4

d. For the design earthquake magnitude with given values of fines content of soil and $(N_1)_{60}$, read off the shear stress ratio required to cause liquefaction from charts shown in Figures 14 through 16. Fines content is defined as the percent of soil particles passing the No. 200 (75 μm) sieve. If the fines content of soil is not greater than 30%, skip Step e and go to Step f.

e. If the fines content of soil is greater than 30%, a correction may be made to the shear stress ratio required to cause liquefaction depending on the plasticity index of soil. If the plasticity index of the soil is greater than 5%, multiply the shear stress ratio required to cause liquefaction by a correlation coefficient ß from Figure 17. For soil with plasticity index not greater than 5%, ß equals one and no correction to the resisting shear stress ratio is needed. The correlation coefficient ß is defined as the ratio between the cyclic strength of soil and the cyclic strength of soil with a plasticity index of 5%.

f. Calculate the safety factor against liquefaction, which is defined as the ratio between the shear stress ratio required to cause liquefaction as obtained from Steps d and e and the induced shear stress ratio computed in Step b. The minimum required factor of safety against liquefaction is 1.1.

The design procedure is demonstrated with a sample problem in Appendix B.

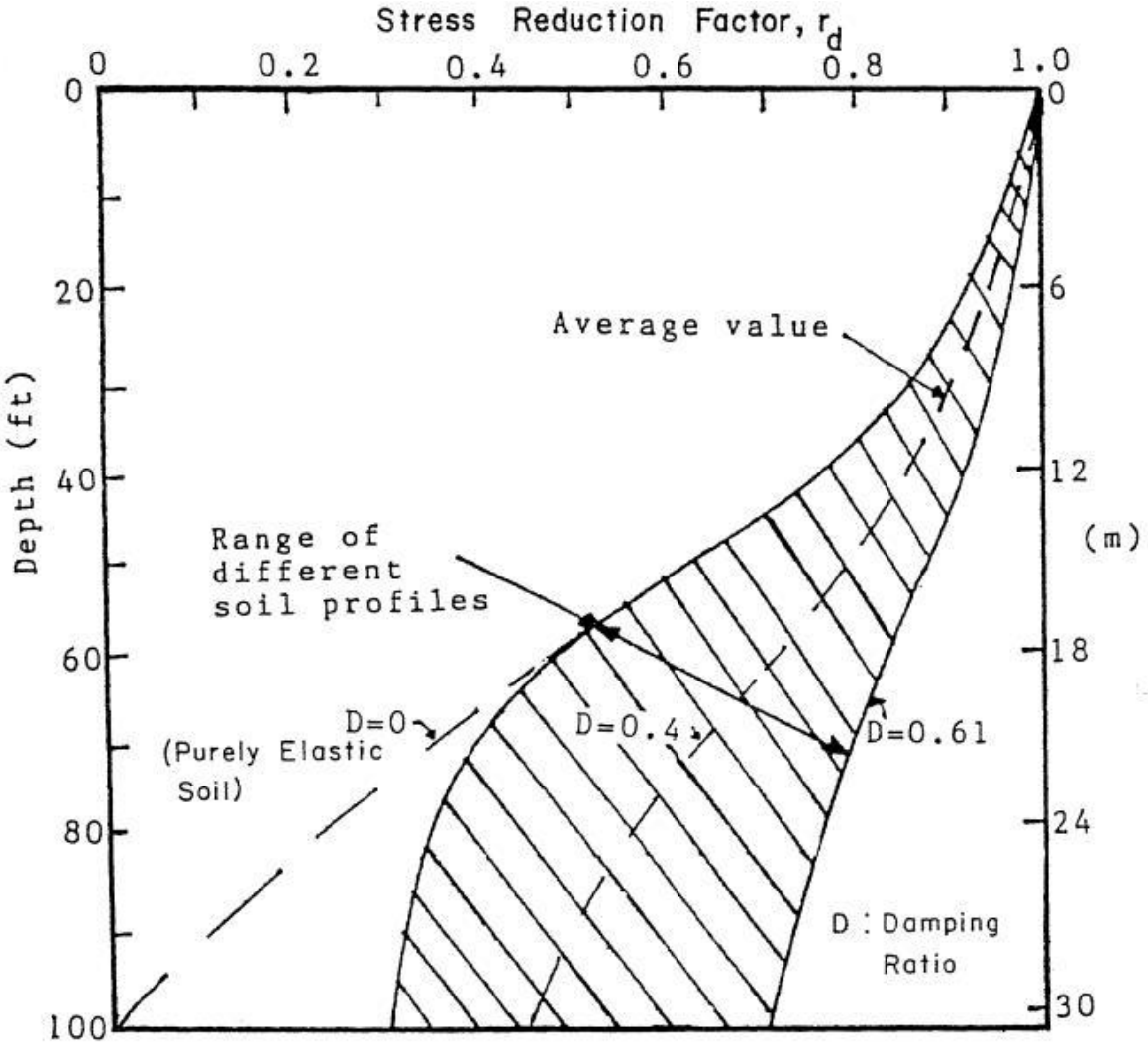

Figure 13 Stress reduction factor in relation to depth (Seed and Idriss, 1971)

TABLE 3
Recommended SPT Procedure for Use in Liquefaction Correlations (Seed et al., 1985)

A. Borehole	4 to 5 in. (10 to 13 cm) diameter rotary borehole with bentonite drilling mud for borehole stability.
B. Drill Bit	Upward deflection of drilling mud (tricone or baffled drag bit)
C. Sampler	O.D. = 3/16 in. (5.00 mm) I.D. = 1/8 in (3.50 mm) – Constant (i.e. no room for liners in barrel)
D. Drill Rods	A or AW for depths less than 50 ft. (15.25 m) N or NW for greater depths
E. Energy Delivered to Sampler	210 lbf·ft (285 Nm) (60% of theoretical maximum)
F. Blow Count Rate	30 to 40 blows per minute
G. Penetration Resistance Count	Measured over range of 6 to 18 in (0.15 to 0.45 m) of penetration into the ground

TABLE 4
Summary of Energy Ratios for SPT Procedures (Seed et al., 1985)

Country	**Hammer Type**	**Hammer Release**	**Estimated Rod Energy (%), ER_m**	**Correction Factor for 60% Rod Energy**
I. Japan**				
	A. Donut	Free Fall	78	78/60 = 1.30
	B. Donut*	Rope & Pulley with special throw release	67	67/60 = 1.12
II. USA	A. Safety*	Rope & Pulley	60	60/60 = 1.00
	B. Donut	Rope & Pulley	45	45/60 = 0.75
III. Argentina	A. Donut*	Rope & Pulley	45	45/60 = 0.75
IV. China	A. Donut*	Free-Fall***	60	60/60 = 1.00
	B. Donut	Rope & Pulley	50	50/60 = 0.83

* Prevalent method in this country today.

** Japanese SPT results have additional corrections for borehole diameter and frequency effects.

*** Pilcon Type hammers, developing an energy ratio of about 60%.

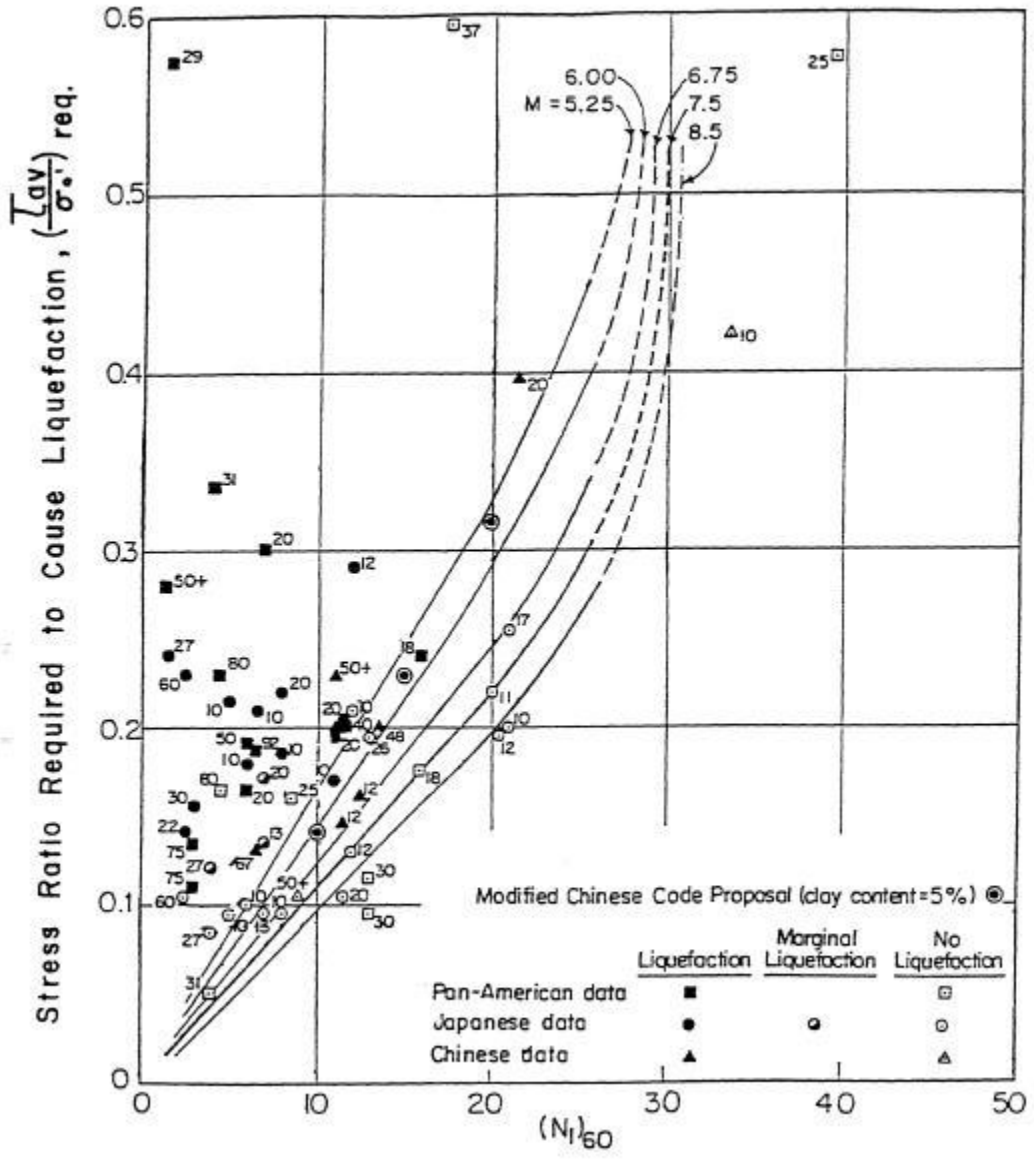

Figure 14 Relationship between stress ratios required to cause liquefaction and $(N_1)_{60}$ values for cohesionless soils having fines content less than 5% in M=5.25-8.5 earthquakes (Seed et al., 1985)

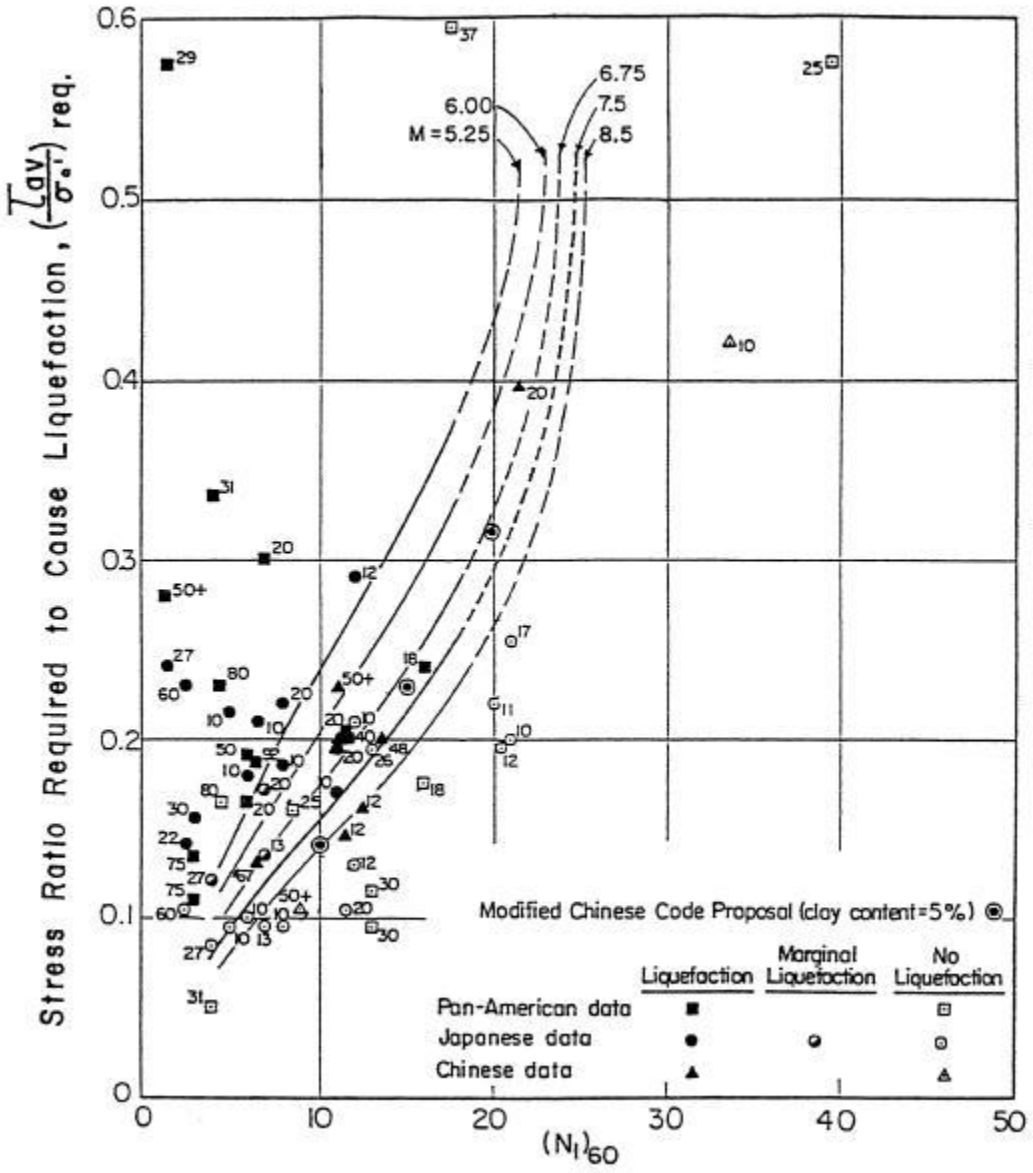

Figure 15 Relationship between stress ratios required to cause liquefaction and $(N_1)_{60}$ values for cohesionless soils having fines content of 15% in M=5.25-8.5 earthquakes (Seed et al., 1985)

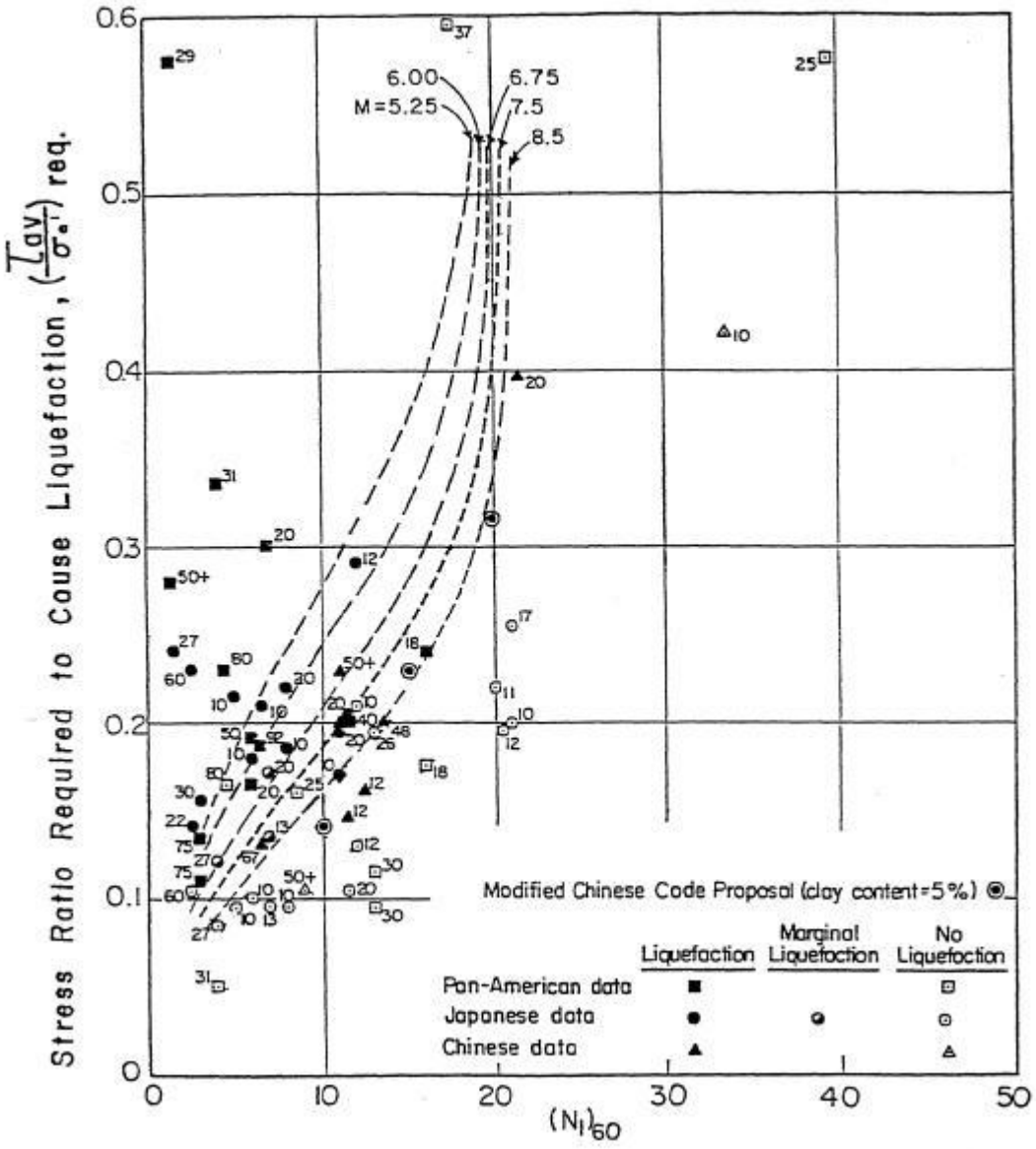

Figure 16 Relationship between stress ratios required to cause liquefaction and $(N_1)_{60}$ values for cohesionless soils having fines content of 35% in M=5.25-8.5 earthquakes (Seed et al., 1985)

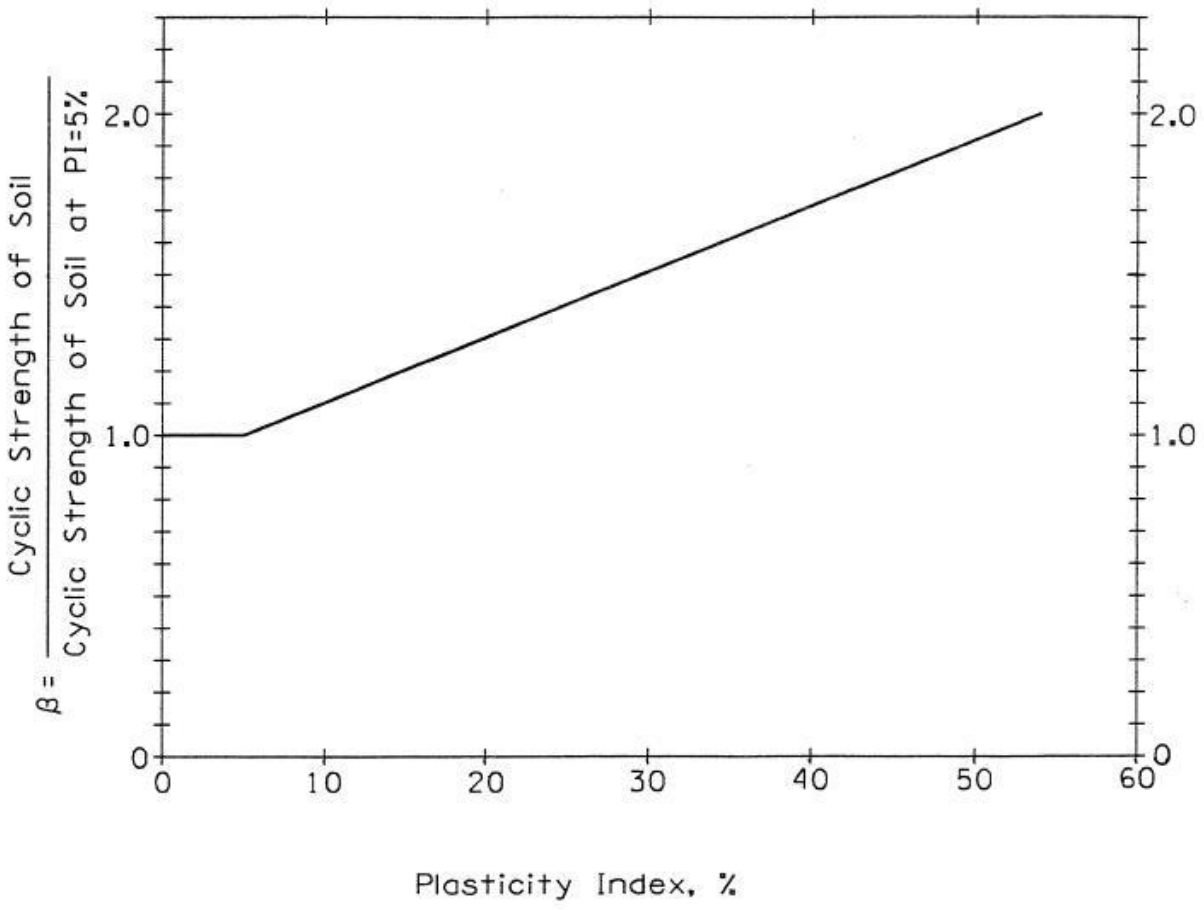

Figure 17 Effect of plasticity index on the cyclic resistance of soil (Ishihara, 1990)

3.2.2 Gravelly Soils

Little information is available on the characteristic and field performance of gravelly soils such as gravelly sands and sandy gravels. As a result, there is no well accepted procedure for evaluating their resistance to liquefaction. However, for preliminary evaluation purposes, the following procedure may be used until a predictive procedure for these soils is available:

a. Determine the soil particle size at 20 percent finer by weight, D_{20}. If D_{20} > No. 35 (0.6 mm), no liquefaction is expected to develop, provided there are no overlying or intervening layers of low permeability soils to inhibit drainage.

b. If D_{20} # No. 35 (0.6 mm), follow Step b of Section 3.2.1 to compute the average induced cyclic shear stress ratio.

c. Follow Step c of Section 3.2.1 to obtain either the average $(N_1)_{60}$ value of sand layers at sites in the vicinity of the gravelly soil deposit in question is considered to have been formed under identical geological conditions or the $(N_1)_{60}$ value of a sand layer, in the same drill hole, immediately above or below the gravelly layer.

d. Follow Steps d and e of Section 3.2.1 to obtain the shear stress ratio required to cause liquefaction.

e. Multiply the shear stress ratio required to cause liquefaction by a correlation coefficient α from Figure 18 to obtain the corrected shear stress ratio required to cause liquefaction for gravelly soils. The correlation coefficient α depends on the gravel content of soil and is defined as the ratio between the cyclic strength of gravelly sand and the cyclic strength of sand with zero percent of gravel.

f. Calculate the safety factor against liquefaction, which is defined as the ratio between the corrected shear stress ratio required to cause liquefaction as obtained from Step d or e and the induced shear stress ratio computed in Step b.

3.3 A Simplified Steady-State Strength Procedure for Analyzing Stability of Embankments and Slopes Against Flow Failures

While the steady-state strength approach is theoretically well founded and has drawn wide attention in the geotechnical profession, the evaluation procedure is still in the developmental stage with some uncertainties remaining (Konrad, 1990; Vasquez-Herrera and Dobry, 1989; Seed et al., 1989; Kramer, 1989; Riemer et al., 1990). In view of these, Seed (1987), De Alba et al. (1988) and Seed et al. (1989), based on investigations of a number of case histories of embankment slope failures involving liquified materials, have developed a correlation between the residual strength or steady-state strength of the liquefied sands and the equivalent clean sand $(N_1)_{60}$ values for the soils involved, as shown in Figure 19. A simplified procedure using this empirical curve for stability against flow failures can be summarized in the following steps:

a. Evaluate the liquefaction potential of each cohesionless soil layer in question in accordance with the procedure as detailed in Section 3.2.1. If the analysis indicates vulnerability to liquefaction, potential stability problems due to flow failure exist. Follow the next step and

complete the stability analysis. If the soil layers are nonliquefiable, no stability problem is anticipated, and stop the analysis.

b. For liquefied sands having more than 5 percent of fines, correct the penetration blow count to an equivalent clean sand blow count by adding an increment, $\Delta(N_1)_{60}$, to the $(N_1)_{60}$ value obtained from Step c of Section 3.2.1 (see Figure 20). This is due to the fact that, even for equal conditions of pore pressure generation-resistance or relative density, the penetration resistance of silty sands and sandy silts is lower than that for clean sands.

c. For the equivalent clean sand $(N_1)_{60}$, read off the liquefied undrained residual strength of sands from Figure 19.

d. Assign the appropriate shear strength parameters to other soil layers: peak drained strengths for nonliquefiable cohesionless soils, peak undrained shear strength for non-sensitive and medium-sensitive plastic soils (sensitivity index less than four), and residual shear strengths for sensitive plastic soils (sensitivity index greater than four).

e. Perform a static slope stability analysis to determine the factor of safety against flow failure. If it is greater than 1, the slope is assumed to be invulnerable to flow slide.

The use of the procedure is illustrated by a sample problem in Appendix C.

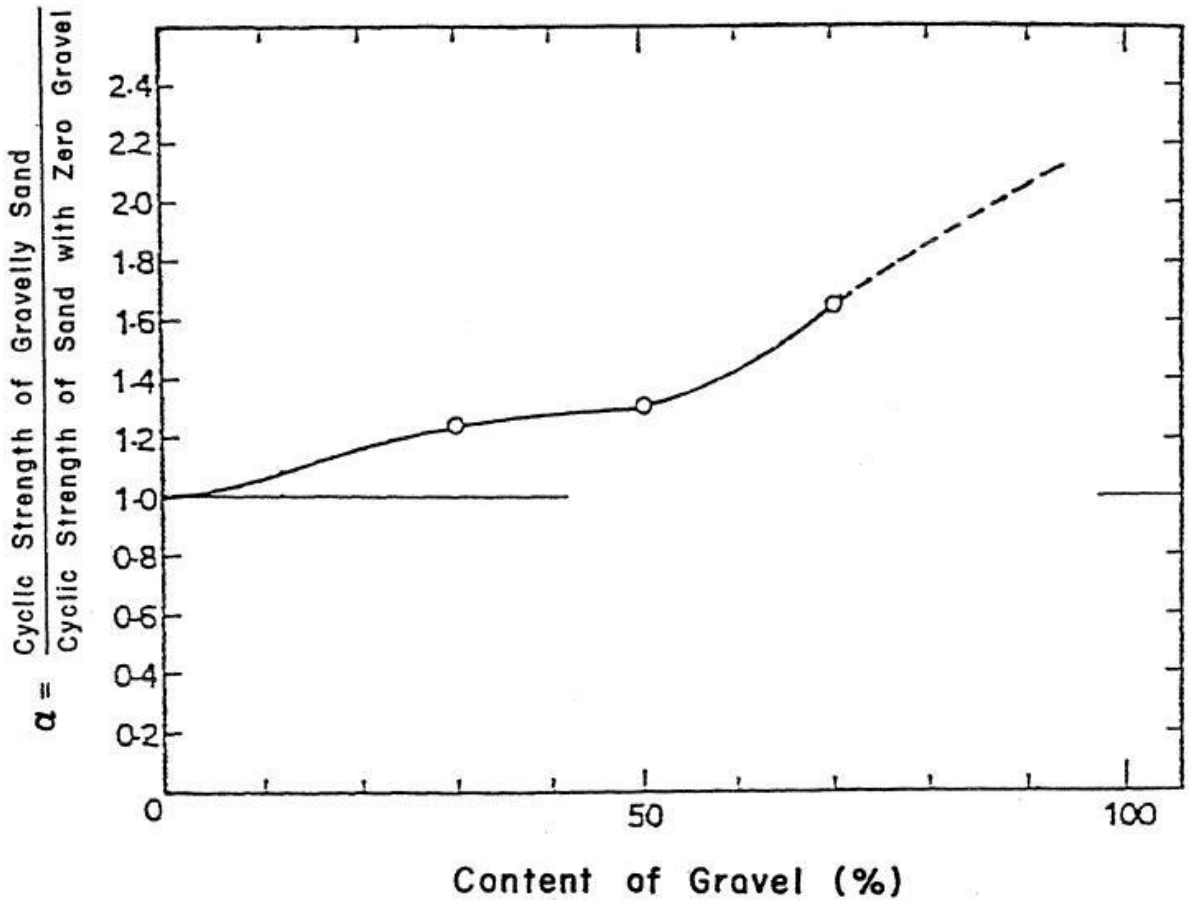

Figure 18 Effects of gravel content on the cyclic resistance of gravelly soils (Ishihara, 1985)

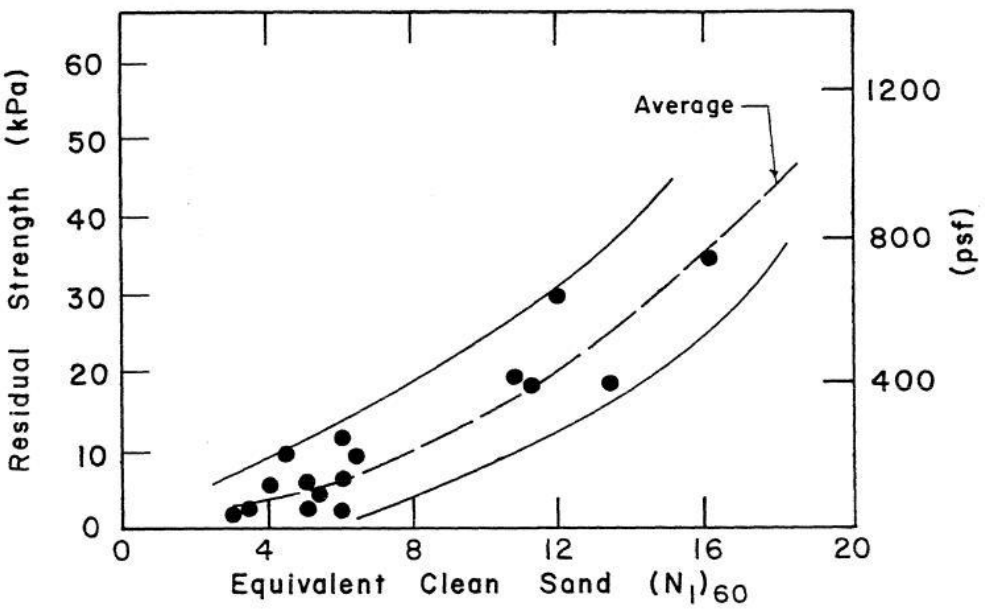

Figure 19 Relationship between residual strength and $(N_1)_{60}$ for sands (Seed et al., 1985)

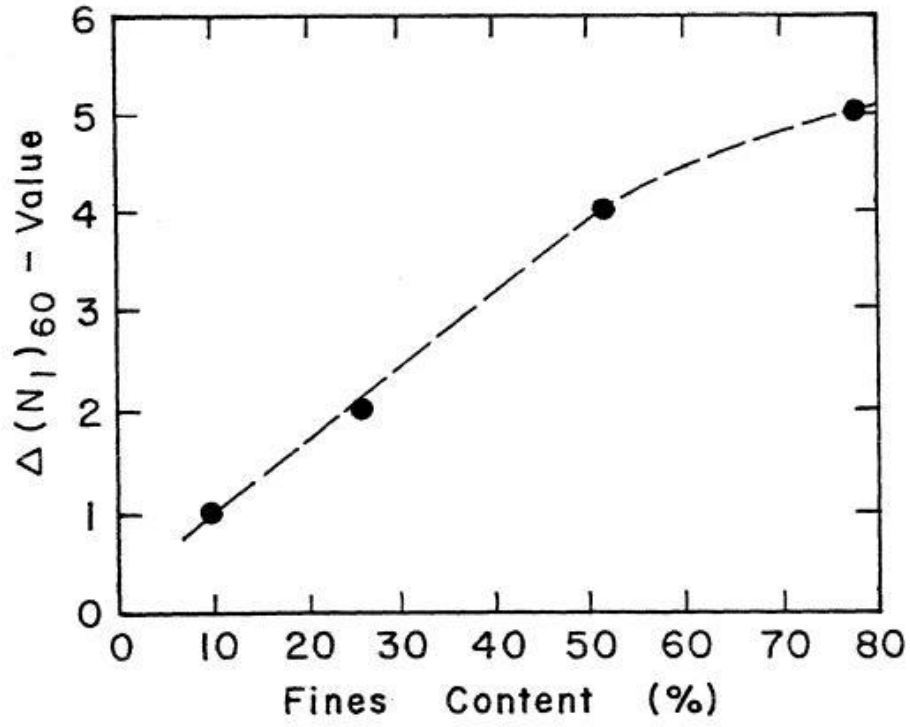

Figure 20 $(N_1)_{60}$ value correction versus fines content for cohesionless soils (Seed et al., 1985)

3.4 Estimation of Earthquake-Induced Settlements in Sands and Sandy Silts

Liquefaction of saturated loose cohesionless soils is always accompanied by ground settlements as the excess pore pressures generated during the earthquake shaking dissipate. The settlement is typically completed within seconds to about one day after the shaking depending on the characteristics of the soil and the length of the drainage path. Post liquefaction settlements as high as 2-3% of the sand layer thickness for loose to medium sands and more than 5% for very loose sands have been reported.

Even though the factor of safety against liquefaction is greater than 1.1 and liquefaction may not occur in cohesionless soil deposits, some pore pressure may be generated and partial liquefaction may occur in these deposits during the earthquake shaking. The dissipation of the pore pressure may result in small amounts of settlement. If the factor of safety against liquefaction is greater than 1.25, the effect of settlement due to partial liquefaction is likely to be insignificant for structures and no settlement analysis is needed. If the factor of safety is less than 1.25, perform a settlement analysis following the procedure described below.

Tokimatsu and Seed (1987) compiled laboratory test data from studies reported by other researchers on the pre-liquefaction and post-liquefaction volumetric strain behavior of saturated clean sands, and concluded that the primary factors controlling the settlement in saturated sands are the cyclic stress ratio and the maximum shear strain induced by the earthquake shaking. Based upon these studies and field observations, they have established a chart, as shown in Figure 21, for an M=7.5 magnitude earthquake, which indicates that the induced volumetric strain is a function of the cyclic stress ratio and $(N_1)_{60}$. This figure is applicable only for sands that have no more than 5% in fines. The simplified procedure for estimating the amount of settlement in clean sands may be described as follows:

1. For each potentially liquefiable layer as identified by the procedure stated in Section 3.2.1, transfer the value of the cyclic stress ratio induced at the design earthquake magnitude to the equivalent cyclic stress ratio value for an M=7.5 event using the following relationship:

$$(\tau_{av} / \sigma_o')_{\text{induced by an M=7.5 earthquake}} = (\tau_{av} / \sigma_o')_{\text{induced by an M=design magnitude earthquake}} \cdot (1/\gamma_m) \qquad \text{Eq(6)}$$

   where γ_m is the correction factor that has the values shown in Figure 22.

2. With the calculated values of $(N_1)_{60}$ and τ_{av}/σ_o' induced at M=7.5, estimate amount of volumetric strain, ε_v, from Figure 21.

3. The total liquefaction induced settlement can be obtained by summing up the contributions of $\varepsilon_v H$ of all potentially liquefiable soil layers, where H is the layer thickness.

No design chart is currently available for estimating the settlement in silty sands and silts. However, in a case study on the geotechnical aspects of the Loma Prieta earthquake by O'Rourke et al. (1991), it was found that using Figure 21 along with the aforementioned procedure overestimated the settlements which occurred in the silty sand fills in San Francisco during this

earthquake by about 100%. For preliminary estimation purposes, the amount of settlement in silty sands and silts may be assumed to be half of that estimated by the aforementioned procedure for clean sands. The use of the procedure for estimating seismically induced settlements in liquefied and partially liquefied sands is illustrated in Appendix B.

Settlements can also occur in loose dry and unsaturated sands due to seismic compaction, but much smaller than those associated with liquefaction in saturated sands. It was found by Silver and Seed (1971) that, for a given soil density and number of seismic cycles, settlement of dry and unsaturated sands due to cyclic loading is not significantly affected by the value of the vertical stress but depends only on the shear strain amplitude in the soil. The maximum volumetric strain induced by an M=7.5 earthquake in dry and unsaturated sands is about 0.5%. For practical purposes, it is assumed that for ordinary bridge projects using a design earthquake magnitude of 6 or less, the amount of settlement in dry and unsaturated sands is very small and can be neglected in foundation design. However, for projects involving bridges that provide critical services, and are settlement sensitive, a special settlement analysis using the procedures proposed by Seed and Silver (1972), Pyke et al. (1975) and Tokimatsu and Seed (1987) may be performed.

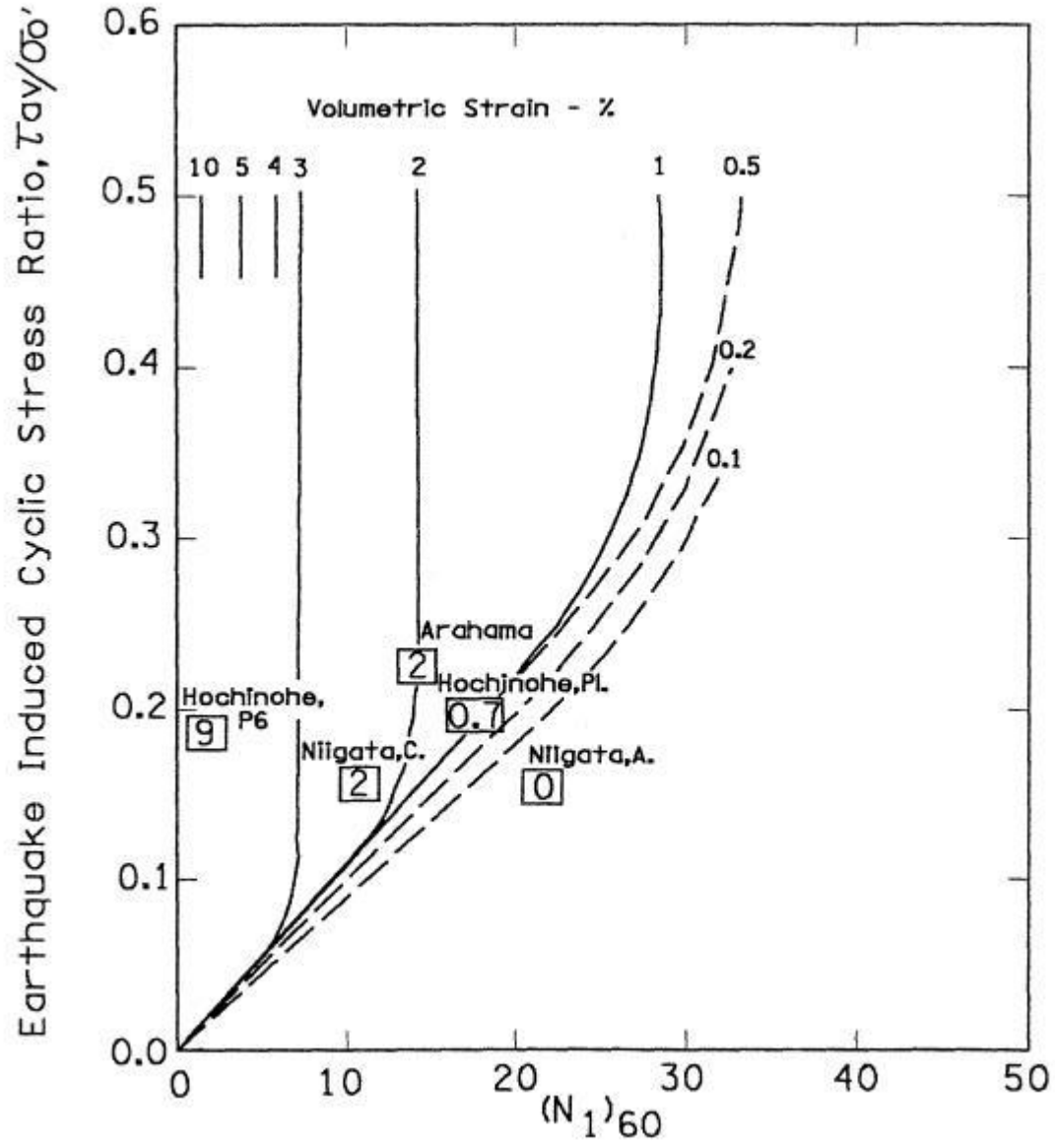

Figure 21 Relationship between cyclic stress ratio, volumetric strain and $(N_1)_{60}$ (Tokimatsu and Seed, 1987)

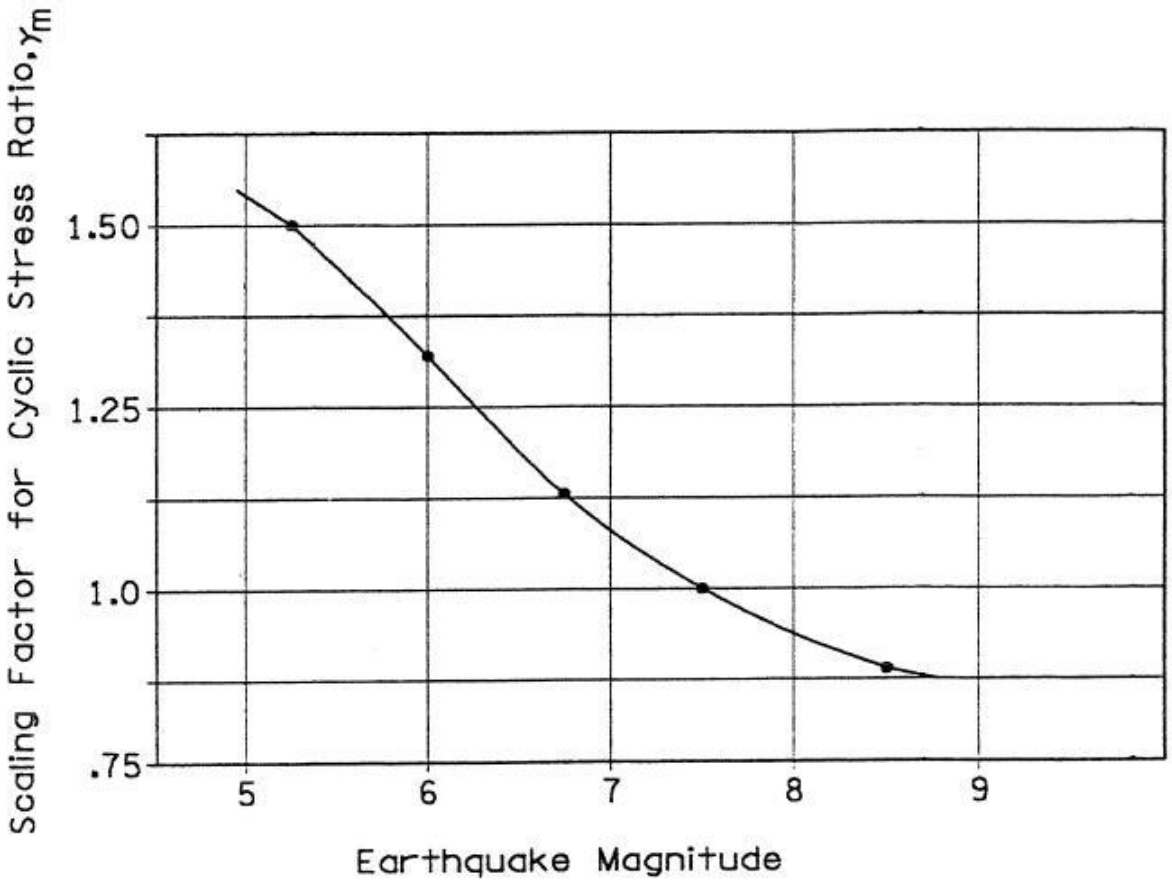

Figure 22 Scaling factor for effect of earthquake magnitude on cyclic stress ratio (Tokimatsu and Seed, 1987)

4. METHODS FOR IMPROVING LIQUEFACTION–PRONE SOILS

4.1 Introduction

Numerous case histories on earthquake activities have documented that liquefaction of cohesionless soils is one of the major causes for structure damage and human casualties. However, one can ensure that liquefaction in loose cohesionless soils cannot be triggered if the effective stress of the soil during shaking is always greater than zero. The development of initial liquefaction in dense sands is often of no practical significance, since subsequent straining will decrease the amount of pore pressure generated.

The danger of liquefaction at a site can be significantly reduced or eliminated by (1) dewatering, (2) increasing the in-situ density and, (3) making provisions to reduce the time required for relieving the excess pore water pressures generated by earthquake loading. These, except dewatering, may be best achieved by ground improvement techniques.

4.2 Dewatering

Dewatering increases the effective stress and shear strength and reduces the extent of saturated soil, all of which increase resistance to liquefaction. However, dewatering a foundation soil is not an easy task. It may require continuous pumping and construction of slurry trenches or walls. It may not be cost-effective and may not be feasible in an alluvial deposit.

4.3 Soil Improvement by In-Situ Techniques

If the potentially liquefiable soil layer is located at the ground surface and is not thicker than 11 ½ ft. (3.5 m), the most economical solution may be removal and replacement with properly compacted nonliquefiable soils. However, for liquefaction-prone soil layers located deeper than 11 ½ ft. (3.5 m) from the ground surface, ground modification techniques such as dynamic compaction, vibroflotation, stone columns and grouting may be the optimal solution. Table 5 summarizes the technical considerations for 15 methods to improve potentially liquefiable soil foundation conditions (Ledbetter, 1985). Each method, according to its function, can be classified into at least one of the following categories:

1. In-situ deep compaction
2. Compression
3. Pore pressure relief
4. Injection and grouting
5. Admixture stabilization
6. Soil reinforcement

It should be noted that two of the most important factors for consideration in choosing an improvement method are the verifiability of improvement and stabilization, and the absence of perceivable safety problems during construction.

TABLE 5
Improvement of Liquefiable Soil Foundation Conditions (Ledbetter, 1985)

Method	Principle	Most Suitable Soil Conditions/Types	Maximum Effective Treatment Depth	Economic Size of Treated Areas	Ideal Properties of Treated Materials
In-Situ Deep Compaction					
1. Vibratory probe	Densification by vibration; liquefaction-induced settlement and settlement n dry soil under overburden to produce a higher density.	Saturated or dry clean sand; sand.	65 ft. (20 m) routinely (ineffective above 10-13 ft. (3-4 m) depth); > 100 ft. (30 m) sometimes.	>10,760 ft.^{2} (1000 m^2)	Can obtain relative densities of 80% or more. Ineffective in some sands.
2. Vibroflotation	Densification by vibration and compaction of backfill material of sand or gravel.	Cohesionless soils with less than 20% fines.	> 100 ft. (30 m)	>10,760 ft.^{2} (1000 m^2)	Can obtain high relative densities (over 85%), good uniformity.
3. Compaction piles	Densification by displacement of pile volume and by vibration during driving, increase in lateral effective earth pressure.	Loose sandy soils; partly saturated clayey soils; loess.	> 65 ft. (20 m)	>10,760 ft.^{2} (1000 m^2)	Can obtain high densities, good uniformity. Relative densities of more than 80%.
4. Dynamic Compaction	Repeated application of high-intensity impacts at surface.	Cohesionless soils best, other types can also be improved.	> 65 ft. (20 m) possible	35,520 ft.^{2} (3300 m^2)	Can obtain high relative densities, reasonable uniformity.

TABLE 5 (cont.)
Improvement of Liquefiable Soil Foundation Conditions (Ledbetter, 1985)

Method	Principle	Most Suitable Soil Conditions/Types	Maximum Effective Treatment Depth	Economic Size of Treated Areas	Ideal Properties of Treated Materials
Compression					
5. Displacement/ Compaction grout	Highly viscous grout acts as radial hydraulic jack when pumped in under high pressure.	All soils.	Unlimited	Small	Grout bulbs within compressed soil matrix. Soil mass as a whole is strengthened.
6. Surcharge/ Buttress	The weight of a surcharge/buttress increases the liquefaction resistance by increasing the effective continuing pressures in the foundation.	Can be placed on any soil surface.	--	>10,760 ft.^{2} (1000 m^2)	Increase strength and reduce compressibility.
Pore Water Pressure Relief					
7. Gravel Drains	Relief of excess pore water pressure to prevent liquefaction.	Sand, silt, clay.	> 100 ft. (30 m)	>16,150 ft.^{2} (1500 m^2)	Fast relief of excess pore water pressure will prevent liquefaction.
Injection and Grouting					
8. Particulate grouting	Penetration grouting-fill soil pores with soil, cement, and/or clay.	Medium to coarse sand and gravel.	Unlimited.	Small	Impervious, high strength with cement grout. Voids filled so they cannot collapse under cyclic loading.

TABLE 5 (cont.)
Improvement of Liquefiable Soil Foundation Conditions (Ledbetter, 1985)

Method	Principle	Most Suitable Soil Conditions/Types	Maximum Effective Treatment Depth	Economic Size of Treated Areas	Ideal Properties of Treated Materials
9. Chemical grouting	Solutions of two or more chemicals react in soil pores to form a gel or a solid precipitate.	Medium silts and coarser.	Unlimited	Small	Impervious, low to high strength. Voids filled so they cannot collapse under cyclic loading.
10. Pressure-injected lime	Penetration grouting – fill soil pores with lime.	Medium to coarse sand and gravel.	Unlimited	Small	Impervious to some degree. No significant strength increase. Collapse of voids under cyclic loading reduced.
11. Electrokinetic injection	Stabilizing chemicals move into and fill soil pores by electro-osmosis or colloids into pores by electro-phoresis.	Saturated sands, silts, silty clays.	Unknown	Small	Increased strength, reduced compressibility, voids filled so they cannot collapse under cyclic loading.
12. Jet grouting	High-speed jets at depths excavate, inject, and mix a stabilizer with soil to form columns or panels.	Sands, silts, clays.	Unknown	Small	Solidified columns and walls.

TABLE 5 (cont.)
Improvement of Liquefiable Soil Foundation Conditions (Ledbetter, 1985)

Method	Principle	Most Suitable Soil Conditions/Types	Maximum Effective Treatment Depth	Economic Size of Treated Areas	Ideal Properties of Treated Materials
Admixture Stabilization					
13. Mix-in-place piles and walls	Lime, cement, or asphalt introduced through rotating auger or special in-place mixer.	Sand, silt, clays, all soft or loose inorganic soils.	> 65 ft. (20 m) (200 ft. (60 m) obtained in Japan)	Small	Solidified soil piles or walls of relatively high strength.
Soil Reinforcement					
14. Vibro-replacement stone and sand columns A. Grouted B. Not grouted	Hole jetted into fine-grained soil and backfilled with densely compacted gravel or sand; hole formed in cohesionless oils by vibro techniques and backfilled with compacted gravel or sand. For grouted columns, voids filled with a grout.	Sands, silts, clays.	> 100 ft. (30 m) (limited by vibratory equipment)	>16,150 ft.^{2} (1500 m^2); fine-grained soils, >10,760 ft.^{2} (1000 m^2)	Increased vertical and horizontal load carrying capacity. Density increase in cohesionless soils. Shorter drainage paths.
15. Root piles, soil nailing	Small-diameter inclusion used to carry tension, shear and compression.	All soils.	Unknown	Unknown	Reinforced zone of soil behaves as a coherent mass.

ACKNOWLEDGEMENTS

This report was prepared by J. Teh Sung. It has benefited from reviews by A. R. Schnore of this Bureau and Klaus Jacob of the Lamont-Doherty Geological Observatory of Columbia University, and from discussions with Walter Mitronovas of the New York State Geological Survey, Ricardo Dobry of Rensselaer Polytechnic Institute, and Martitia Tuttle of the Lamont-Doherty Geological Observatory.

REFERENCES

Algermissen, S. T., Perkins, D. M., Thenhaus, P. C., Hanson, S. L., and Bender, B. L., "Probabilistic Estimates of Maximum Acceleration and Velocity in Rock in the Contiguous United States," U. S. Geological Survey, Open File Report 82-1033, 1982.

Algermissen, S. T., Perkins, D. M., Thenhaus, P. C., Hanson, S. L., and Bender, B. L., "Probabilistic Earthquake Acceleration and Velocity Maps for the United States and Puerto Rico," Miscellaneous Field Studies Map MF-2120, U. S. Geological Survey, 1990.

Anderson, L. R., Keaton, J. R., Aubry, K., and Ellis, S. J., "Liquefaction Potential Map for Davis County, Utah," Department of Civil and Environmental Engineering, Utah State University, Logan, Utah, 1982.

Andrus, R. D., Stokoe, K. H., and Roesset, J. M., "Liquefaction of Gravelly Soil at Pence Ranch During the 1983 Borah Peak, Idaho Earthquake," First International Conference on Soil Dynamics and Earthquake Engineering V, Karlsruhe, Germany, September 1991.

Arulanandan, K., "Method and Apparatus for Measuring In-Situ Density and Fabric Soils," patent application, Regents of the University of California, Berkeley, California, 1977.

Arulmoli, K., Arulanandan, K., and Seed, H. B., "New Method for Evaluating Liquefaction Potential," Journal of the Geotechnical Engineering Division, ASCE, Vol. 111, No. GT1, 1985.

Baldi, G., Bellotti, R., Ghionna, V., Jamiolkowski, M., and Pasqualini, E., "Penetration Resistance and Liquefaction of Sands," Proceedings of the 11th International Conference on Soil Mechanics and Foundation Engineering, San Francisco, 1985.

Barosh, P. J., "Earthquake Controls and Zonation in New York," Proceedings of Conference XXIV, U.S. Geological Survey, Open File 85-386, 1984.

Bartlett, S. F., and Youd, T. L., "Empirical Analysis of Horizontal Ground Displacement Generated by Liquefaction-Induced Lateral Spreads," Report No. NCEER-92-0021, NCEER, SUNY at Buffalo, 1992.

Bierschwale, J. G., and Stokoe, K. H., II, "Analytical Evaluation of Liquefaction Potential of Sands Subjected to the 1981 Westmoreland Earthquake," Geotechnical Engineering Report GR-84-15, Civil Engineering Department, University of Texas, Austin, Texas, 1984.

Campanella, R. G., and Robertson, P. K., "A Seismic Cone Penetrometer to Measure Engineering Properties of Soil," Proceedings of the Fifty-fourth Annual Meeting of the Society of Exploration Geophysicists, Atlanta, Georgia, 1984.

Casagrande, A., "Characteristics of Cohesionless Soils Affecting the Stability of Slopes and Earth Fills," Journal of the Boston Society of Civil Engineers, 1936, reprinted in Contributions to Soil Mechanics, 1925 to 1940, Boston Society of Civil Engineers, Oct., 1940.

Castro, G., "Liquefaction of Sands," Thesis Presented to Harvard University in Fulfillment of the Requirements for the Degree of Doctor of Philosophy, 1969.

Castro, G., "On the Behavior of Soils During Earthquakes - Liquefaction," Proceedings of the 3rd International Conference on Soil Dynamics and Earthquake Engineering, Princeton, New Jersey, June, 1987.

Castro, G., Poulos, S. J., France, J. W., and Enos, J. L., "Liquefaction Induced by Cyclic Loading," Report to National Science Foundation, Geotechnical Engineers, Inc., Winchester, Massachusetts, 1982.

Chameau, J. L., and Clough, G. W., "Probabilistic Pore Pressure Analysis for Seismic Loading," Journal of the Geotechnical Engineering Division, ASCE, Vol. 109, No. GT4, 1983.

De Alba, P. A., Seed, H. B., Retamal, E., and Seed, R. H., "Analysis of Dam Failures in 1985 Chilean Earthquake," ASCE, Journal of the Geotechnical Engineering Division, ASCE, Vol. 114, No. GT12, 1988.

Dobry, R., "Some Basic Aspects of Soil Liquefaction During Earthquakes," Proceedings of the Conference on Earthquake Hazards and the Design of Constructed Facilities in the Eastern United States, Academy of Sciences, New York, Feb. 24-26, 1989.

Dobry, R., Powell, D. J., Yokel F. Y., and Ladd, R. S., "Liquefaction Potential of Saturated Sand - The Stiffness Methods," Proceedings of the 7th World Conference on Earthquake Engineering, Istanbul, Vol. 3, 1980.

Dobry, R., and Vucetic, M., "Dynamic Properties and Seismic Response of Soft Clay Deposits," Proceedings of the International Symposium on Geotechnical Engineering of Soft Soils, Mexico, Vol. 2, Session 1B, 1987.

Dobry, R., Yokel, F. Y., and Ladd, R. S., "Liquefaction Susceptibility from S-Wave Velocity," ASCE National Convention, St. Louis, Missouri, October, 1981.

Douglas, B. J., Olsen, R. S., and Martin, G. R., "Evaluation of the Cone Penetrometer Test for SPT-Liquefaction Assessment," In Situ Testing to Evaluate Liquefaction Susceptibility, Preprint 81-544, ASCE National Convention, St. Louis, Missouri, 1981.

Earthquakes and Volcanoes, "The Loma Prieta, California, Earthquake of October 17, 1989," U.S. Geological Survey, Vol. 21, No. 5, 1989.

Earthquake Information Bulletin, U. S. Geological Survey, Department of the Interior, Washington, D. C., Vol. 7, No.4, July-August, 1975.

Ebel, J.,"The Seismicity of the Northeastern United States," Proceedings of the Symposium on Seismic Hazards, Ground Motions, Soil-Liquefaction and Engineering Practice in Eastern North America, NCEER, SUNY at Buffalo, October, 1987.

Fardis, M. N., and Veneziano, D, "Probabilistic Analysis of Deposit Liquefaction," Journal of the Geotechnical Engineering Division, ASCE, Vol. 108, No. GT3, 1982.

FEMA, "NEHRP Recommended Provisions for the Development of Seismic Regulations for New Buildings," Federal Emergency Management Agency, Earthquake Hazards Reduction Series 17, FEMA 95, October 1988.

Finn, W. D. L., "Liquefaction Potential: Developments Since 1976," Proceedings of the International Conference on Recent Advances in Geotechnical Earthquake Engineering and Soil Dynamics, University of Missouri, Rolla, Missouri, 1981.

Finn, W. D. L., Brandy, P. L., and Pickering, D. L., "Effect of Strain History on Liquefaction of Sand," Journal of the Geotechnical Engineering Division, ASCE, Vol. 96, No. GT6, November, 1970.

Finn, W.D. Liam, Lee, Kwok W., and Martin, Geoffrey R., "An Effective Stress Model for Liquefaction of Sands", Journal of the Geotechnical Engineering Division, ASCE, Vol. 102, No. GT8, 1976.

Fischer, J. A., and McWhorter, J. G., "The Microzonation of New York State," Microzonation Conference for Safer Construction Research and Applications, Seattle, Oct., 1972.

Fuller, M. L., "The New Madrid Earthquake," Bulletin 494, U.S. Geological Survey, Department of Interior, Washington, D.C., 1912.

Geotechnical News, Volume 8, No.1, March, 1990.

Haldar, A., and Tang, W. H., "Probabilistic Evaluation of Liquefaction Potential," Journal of the Geotechnical Engineering Division, ASCE, Vol. 105, No. GT2, 1979.

Idriss, I. M., "Response of Soft Soil Sites During Earthquakes," Proceedings of the Memorial Symposium to Honor Professor Harry Bolton Seed, University of California, Berkeley, May, 1990.

Idriss, I. M., and Seed, H. B., "Seismic Response of Horizontal Soil Layers," Journal of the Soil Mechanics and Foundation Division, ASCE, Vol. 96, No. SM4, 1968.

Ishihara, K., "Stability of Natural Deposits During Earthquakes," Proceedings of the Eleventh International Conference on Soil Mechanics and Foundation Engineering, San Francisco, 1985.

Ishihara, K., "Evaluation of Liquefaction Potential and Consequent Deformations in Sandy Fills," Proceedings of the Seismic Workshop on the Port of Los Angeles, 1990.

Jacob, K. H., "Seismic Hazard in New York City Area," Seminar Notes for the Practical Aspects of Earthquake Engineering, Architecture, and Construction, New York City, May 23, 1991.

Jacob, K. H., "Seismic Hazards in the Eastern U.S. and the Impact on Transportation Lifelines," Proceedings of the Lifeline Earthquake Engineering in the Central and Eastern US, ASCE, New York, September, 1992.

Konard, J. M., "Minimum Undrained Strength of Two Sands," Journal of the Geotechnical Engineering Division, ASCE, Vol. 116, No. GT6, June, 1990.

Kovacs, W. D., Yokel, F. Y., Salomone, L. A., and Holtz, R. D., "Liquefaction Potential and the International SPT," Proceedings of the Eighth World Conference on Earthquake Engineering, Volume 3, Prentice-Hall, Inc., Englewood Cliffs, New Jersey, 1984.

Kramer, S. L., "Uncertainty in Steady-State Liquefaction Evaluation Procedures," Journal of the Geotechnical Engineering Division, ASCE, Vol. 115, No. GT10, October, 1989.

Kulhway, F. H., and Ninyo, A., "Earthquakes and Earthquake Zones in New York State," Bulletin of Association of Engineering Geologists, Vol. XIV, No. 2, 1977.

Law, K. T., "Analysis of Soil Liquefaction During the 1988 Saguenay Earthquake," Proceedings of the 43rd Canadian Geotechnical Conference, Quebec, October 10-12, 1990.

Ledbetter, R. H., "Improvements of Liquefiable Foundation Conditions Beneath Existing Structures," Technical Report REMR-GT-2, U.S. Army Corps of Engineers, Waterways Experiment Station, Vicksburg, Mississippi, 1985.

Lee, K. L., and Fitton, J. A., "Factors Affecting the Cyclic Loading Strength of Soil," Vibration Effects of Earthquakes on Soils and Foundations, ASTM STP 450, American Society for Testing and Materials, 1969.

Liao, S., and Whitman, R. V., "Overburden Correction Factors for SPT in Sand," Journal of the Geotechnical Engineering Division, ASCE, Vol. 112, No. GT3, 1986.

Liao, S., Veneziano, P., and Whitman, R., "Regression Model for Evaluating Liquefaction Probability," Journal of the Geotechnical Engineering Division, ASCE, Vol. 114, No. GT4, 1988.

Lindh, A. G., "Earthquake Prediction Comes of Age," Technology Review, February/March, 1990.

Liou, C. P., Streeter, V. L., and Richart, F. E., "A Numerical Model for Liquefaction," Journal of the Geotechnial Engineering Division, ASCE, No. GT6, 1977.

Martin, P. P., and Seed, H. B., "MASH: A Computer Program for the Nonlinear Analysis of Vertically Propagating Shear Waves in Horizontally Layered Deposits," Report UCB/EERC 78/23, Earthquake Engineering Research Center, University of California, Berkeley, October, 1978.

Mitronovas, W., "Earthquake Statistics in New York State," Earthquake Notes, Vol. 53, No. 2, April-June, 1982.

Mitronovas, W., and Nottis, G. N., "Seismicity of New York: Current Status of Scientific Knowledge and Research in Historical Seismicity," Proceedings of Conference XXIX, U.S. Geological Survey, Open File 85-386, 1984.

National Research Council, "Liquefaction of Soils During Earthquakes," Committee on Earthquake Engineering, National Research Council, National Academy Press, Washington, D.C., 1985.

New York State Geological Survey, "Current Facts About Earthquakes and Earthquake Preparedness in New York," NYSGS, October, 1989.

NCEER, "Fact Sheet," National Center for Earthquake Engineering Research, SUNY at Buffalo, 1990.

O'Rourke, T. D., Gowdy, T. E., Steward, H. E., and Pease, J. W., "Lifeline Performance and Ground Deformation in Marine During the 1989 Loma Prieta Earthquake," Report No.NCEER-90-0001, NCEER, Feb., 1991.

Poulos, S. J., "The Steady State of Deformation," Journal of the Geotechnical Engineering Division, ASCE, Vol. 107, No. GT5, 1981.

Poulos, S. J., Castro, G., and France, J. W., "Liquefaction Evaluation Procedure," Journal of the Geotechnical Engineering Division, ASCE, Vol. 111, No. GT6, 1985.

Poulos, S. J., Robinsky, E. I., and Keller, T. O., "Liquefaction Resistance of Thickened Tailings," Journal of the Geotechnical Engineering Division, ASCE., Vol. 111, No. GT12, 1985.

Prevost, J. H., "DYNAID: A Computer Program for Nonlinear Seismic Site Response Analysis," Technical Report NCEER-89-0025, National Center for Earthquake Engineering Research, SUNY at Buffalo, 1989.

Pyke, R., Seed, H. B., and Chan, C. K., "Settlement of Sands Under Multidirectional Shaking," Journal of the Geotechnical Engineering Division, ASCE, GT4, 1975.

Riemer, M., Seed, R., Nicholson, P., and Jong, H. L., "Steady State Testing of Loose Sands: Limiting Minimum Density," Journal of the Geotechnical Engineering Division, ASCE, Vol. 116, No. GT2, February, 1990.

Robertson, P. K., and Campanella, R. G., "Liquefaction Potential of Sands Using the CPT," Journal of the Geotechnical Engineering Division, ASCE, Vol. 111, No. GT3, 1985.

Robertson, P. K., Campanella, R. G., and Wightman, A., "SPT-CPT Correlations," Journal of the Geotechnical Engineering Division, ASCE, Vol. 109, No. GT11, 1983.

Ross, G. A., Seed, H. B., and Migliaccio, R. R. "Bridge Foundations in Alaska Earthquake," Journal of the Soil Mechanics and Foundation Engineering, ASCE, Vol. 95, No. SM4, July, 1969.

Schnabel, P. B., Lysmer, J., and Seed, H. B., "SHAKE: A Computer Program for Earthquake Response Analysis of Horizontally Layered Sites," Report No. EERC 72-12, University of California, Berkeley, California, December, 1972.

Seed, H. B., "Landslides During Earthquakes," Journal of the Soil Mechanics and Foundations Division, ASCE, Vol. 94, No. SM5, September, 1968.

Seed, H. B., "Soil Liquefaction and Cyclic Mobility Evaluation for Level Ground During Earthquakes," Journal of the Geotechnical Engineering Division, ASCE, Vol. 105, No. GT2, 1979.

Seed, H. B., "Design Problems in Soil Liquefaction," Journal of the Geotechnical Engineering Division, ASCE, Vol. 113, No. GT8, 1987.

Seed, H. B., and Idriss, I. M., "Simplified Procedure for Evaluating Soil Liquefaction Potential," Journal of the Soil Mechanics and Foundation Division, ASCE, Vol. 97, No. SM9, 1971.

Seed, H. B., and Silver, M. L., "Settlement of Dry Sands during Earthquakes," Journal of the Soil Mechanics Foundation Division, ASCE, No. SM4, 1972.

Seed, H. B., Idriss, I. M., and Arango, I., "Evaluation of Liquefaction Potential Using Field Performance Data," Journal of the Geotechnical Engineering Division, ASCE, Vol. 109, No. GT3, 1983.

Seed, H. B., Lee, K. L., Idriss, I. M., and Makdisi, F. I., "The Slides in the San Fernando Dams During the Earthquake of February 9, 1971," Journal of the Geotechnical Engineering Division, ASCE, Vol. 101, No. GT7, July, 1975.

Seed, H. B., Mori, K., and Chan, C. K., "Influence of Seismic History on Liquefaction of Sand," Journal of the Geotechnical Engineering Division, ASCE, Vol. 103, No. GT4, 1977.

Seed, H. B., Muraka, R., Lysmer, J., and Idriss, I., "Relationships of Maximum Acceleration, Maximum Velocity, Distance From Source, and Local Site Conditions for Moderately Strong Earthquakes," Bulletin of the Seismological Society of America, Vol. 66, No. 4, August, 1976.

Seed, H. B., Seed, R. B., Harder, L. F., and Jong, H. L., "Examination of the Post-Earthquake Slide of February 9, 1971," Re-evaluation of the Lower San Fernando Dam Report 2, Department of the Army, U.S. Army Corps of Engineers, Washington, D.C., Contract Report GL-89-2, September, 1989.

Seed, H. B., Tokimatsu, K., Harder, L. F., and Chung, R. M., "Influence of SPT Procedures in Soil Liquefaction Resistance Evaluations," Journal of the Geotechnical Engineering Division, ASCE, Vol. 3, No. GT12, 1985.

Sherif, M. A., Ishibashi, I., and Tsuchiya, C., "Saturation Effects on Initial Soil Liquefaction," Journal of the Geotechnical Engineering Division, ASCE, Vol. 103, No. GT8, 1977.

Silver, M. L., and Seed, H. B., "Volume Changes in Sands During Cyclic Loading," Journal of the Soil Mechanics Foundation Division, ASCE, No. SM9, 1971.

Singh, R. D., Dobry, R., Doyle, E., and Idriss, I., "Nonlinear Seismic Response of Soft Clay Sites," Journal of the Geotechnical Engineering Division, ASCE, Vol. 107, NO. GT9, 1981.

Singh, S., Donovan, N. C., and Park, F., "A Re-examination of the effect of Prior Loadings on the Liquefaction Resistance of Sands," Proceedings of the 8th World Conference on Earthquake Engineering, Vol. 3, Istanbul, Turkey, September, 1980.

Tinsley, J. C., Youd, T. L., Perkins, D. M., and Chen, A. T. F., "Evaluating Liquefaction Potential," Evaluating Earthquake Hazards in the Los Angeles Region, an Earth Science Perspective, Professional Paper 1360, J. I. Ziony, Ed., U.S. Geological Survey, 1985.

Tokimatsu, K., and Seed, H. B., "Evaluation of Settlement in Sands due to Earthquake Shaking," Journal of the Geotechnical Engineeering Division, N0. GT8, 1987.

Tokimatsu, K., and Yoshimi, Y., "Empirical Correlation of Soil Liquefaction Based on SPT N-Value and Fines Content," Soils and Foundations, Japanese Society of Soil Mechanics and Foundation Engineering, Vol. 23, No. 4, 1983.

Tsuchida, H., "Prediction and Countermeasure Against the Liquefaction in Sand Deposits," Abstract of the Seminar in the Port and Harbor Research Institute (in Japanese), 1970.

Tuttle, M., and Seeber, L., "Earthquake-Induced Liquefaction in the Northeastern United States: Historical Effects and Geological Constraints," Proceedings of the Conference on Earthquake Hazards and Design of Construction Facilities in the Eastern United States, Academy of Sciences, New York, Feb. 24-26, 1989.

Varnes, D. J., "Slope Movements and Processes," Landslides - Analysis and Control, National Academy of Sciences, Washington, D.C., Special Report 176, 1978.

Vasequez-Herrera, A., and Dobry, R., "The Behavior of Undrained Contractive Sand and its Effect on Seismic Liquefaction Flow Failures of Earth Structures," Re-evaluation of the Lower San Fernando Dam Report 3, Rensselaer Polytechnic Institute, prepared for Department of the Army, U.S. Corps of Engineers, Washington, D.C., Contract Report GL-89-2, September, 1989.

Walker, A.J., and Steward, H.E., "Cyclic Undrained Behavior of Nonplastic and Low Plasticity Silts," Technical Report NCEER-89-0035, National Center for Earthquake Engineering Research, SUNY at Buffalo, July 26, 1989.

Whitman, R. V., "On Liquefaction," Proceedings of the Eleventh International Conference on Soil Mechanics and Foundation Engineering, San Francisco, 1985.

Yegian, M., and Whitman, R. V., "Risk Analysis for Ground Failure by Liquefaction," Journal of the Geotechnical Engineering Division, ASCE, Vol. 104, No. GT7, 1978.

Youd, T. L., "Geologic Effects - Liquefaction and Associated Ground Failure," Proceedings of the Geologic and Hydrologic Hazards Training Program, Open-File Report 84-760, U.S. Geological Survey, Menlo Park, California, 1984.

Youd, T. L., and Hoose, S. N., "Liquefaction Susceptibility and Geologic Setting," Proceedings of the Sixth World Conference on Earthquake Engineering, Volume 3, Prentice-Hall, Inc., Englewood Cliffs, New Jersey, 1977.

Youd, T. L., and Perkins, M., "Mapping Liquefaction-Induced Ground Failure Potential," Journal of the Geotechnical Engineering Division, ASCE, Vol. 104, No. GT4, 1978.

Youd, T. L., and Perkins, M., " Mapping of Liquefaction Severity Index," Journal of the Geotechnical Engineering Division, ASCE, Vol. 113, No. GT11, 1987.

Youd, T. L., Tinsley, J. C., Perkins, D. M., King, E. J., and Preston, R. F., "Liquefaction Potential Map of San Fernando Valley, California," Proceedings of the Second International Conference on Microzonation for Safety Construction - Research and Applications, Volume 1, National Science Foundation, Washington, D.C., 1978.

Zoback, M. D., "In Situ Stress, Crustal Strain and Seismicity in Eastern North America," Proceedings of the Symposium on Seismic Hazards, Ground Motions, Soil-Liquefaction and Engineering Practice in Eastern North America, Edited by K. H. Jacob, Technical Report NCEER-87-0025, NCEER, SUNY at Buffalo, December, 1987.

APPENDIX

APPENDIX A

Modified Mercalli Intensity and Richter Scale Magnitude

The severity of an earthquake can be expressed in terms of both intensity and magnitude. However, the two terms have quite different meanings as described below.

Intensity

The effect of an earthquake on the Earth's surface is called the intensity. It is generally expressed by scales describing a subjective evaluation at the place of observation of the destructiveness from the energy released at the earthquake focus. Although numerous intensity scales have been developed over the last several hundred years, the one currently used in the United States is the Modified Mercalli Intensity scale, MMI, developed in 1931 by Harry Wood and Frank Neumann. This scale ranks the shaking levels in an ascending order from I to XII. A condensed version of the MMI scale is given in Table A.1. Sand boils and ground failures resulting from liquefaction are generally assigned to MMI level VIII and higher.

The MMI generally decreases with the distance from the earthquake epicenter. However, the intensity of ground shaking at a given site is a complex function of many factors, such as size of the earthquake at focus, site distance to the earthquake epicenter, type and thickness of the soil and rock deposits that underlie the site, attenuation, soil amplification, soil-structure interaction, etc. Therefore, the earthquake intensity level at a given site may vary considerably from that observed a short distance away. For example, an assessment of the distribution of MMI resulting from the Loma Prieta earthquake is shown in Figure A.1. (Earthquakes and Volcanoes, 1989). It can be seen that the estimated intensity levels in western Oakland and eastern and northern San Francisco, where alluvium and soft clay are deposited, are one to three units higher than in other areas of the cities.

APPENDIX A

TABLE A.1
Modified Mercalli Scale

I.	Not felt except by a very few under especially favorable circumstances.
II.	Felt only by a few persons at rest, especially on upper floors of buildings. Suspended objects may swing slightly.
III.	Felt quite noticeably indoors, especially on upper floors of buildings, but many people do not recognize it as an earthquake. Standing motor cars may rock slightly. Vibration like passing truck. Duration estimated.
IV.	During the day felt indoors by many, outdoors by few. At night some awakened. Dishes, windows, doors disturbed; walls make creaking sound. Sensation like heavy truck striking building. Standing motor cars rocked noticeably.
V.	Felt by nearly everyone; many awakened. Some dishes, windows, etc. broken; a few instances of cracked plaster; unstable objects overturned. Disturbances of trees, poles. And other tall objects sometimes noticed. Pendulum clocks may stop.
VI.	Felt by all; many are frightened and run outdoors. Some heavy furniture moved; a few instances of fallen plaster or damaged chimneys. Damage slight.
VII.	Everybody runs outdoors. Damage negligible in buildings of good design and construction; slight to moderate in well-built ordinary structures; considerable in poorly built or badly designed structure; some chimneys broken. Noticed by persons driving motor cars.
VIII.	Damage slight in specially designed structures; considerable n ordinary substantial buildings with partial collapse; great in poorly built structures. Panel walls thrown out of frame structures. Fall of chimneys, factory stacks, monuments, walls. Heavy furniture overturned. Sand and mud ejected in small amounts. Changes in well water. Persons driving motor cars disturbed.
IX.	Damage considerable in specially designed structures; well designed frame structures thrown out of plumb; great in substantial buildings, with partial collapse. Buildings shifted off foundations. Ground cracked conspicuously. Underground pipes broken.
X.	Some well-built wooden structures destroyed; most masonry and frame structures destroyed with foundations; ground badly cracked. Rails bend. Landslides considerable from river banks and steep slopes. Shifted sand and mud. Water splashed (slopped) over banks.
XI.	Few, if any, (masonry) structures remain standing. Bridges destroyed. Broad fissures in ground. Underground pipe lines completely out of service. Earth slumps and land slips in soft ground. Rails bent greatly.
XII.	Damage total. Waves seen on ground surfaces. Lines of sight and level distorted. Objects thrown upward into the air.

APPENDIX A

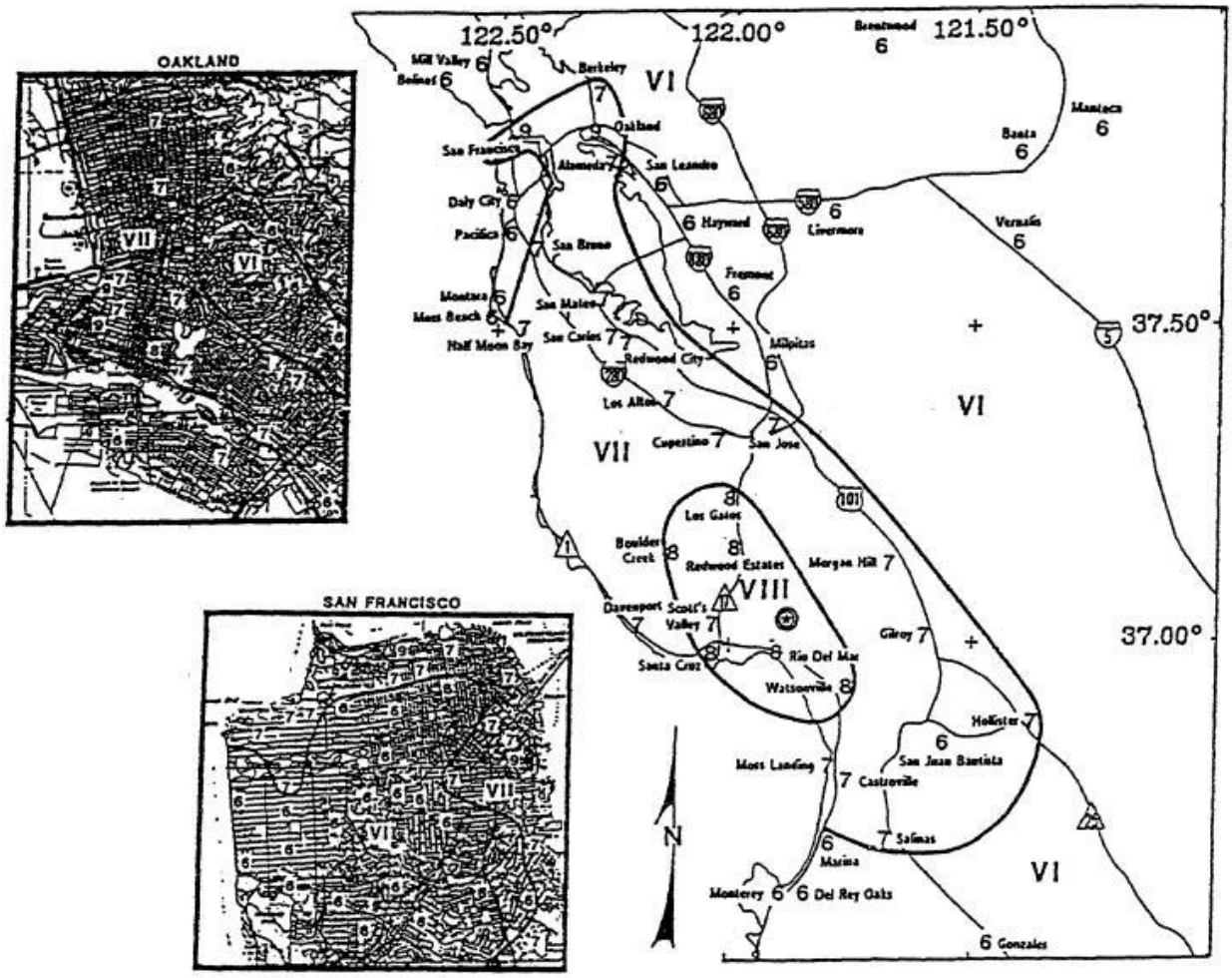

Figure A.1 The modified Mercalli intensity levels for the Loma Prieta earthquake (Earthquake & Volcanoes, 1989)

APPENDIX A

Magnitude

Magnitude is related to the amount of seismic energy released at the hypocenter of the earthquake. Richter magnitude is based on the amplitude of the seismic waves recorded on instruments called seismographs. These devices may amplify ground motions beneath the instruments to over one million times, transcribing the motion into a zig-zag trace called a seismogram. From the data expressed in seismograms, the time, epicenter and focal depth of an earthquake can be determined and estimates can be made of its relative size and the amount of energy that was released.

When Richter and Gutenberg first introduced the earthquake scales in 1933 for local magnitude, M_L, surface wave magnitude, M_S, and body-wave magnitude, m_b, they intended that all three scales would give the same number for a given earthquake. However, the scales do not yield the same number because the shape of the ground motion spectrum changes as the size of the earthquake changes. M_L defines the magnitude as the logarithm of the maximum amplitude, in microns, traced on a seismograph at a distance of 60 miles (100 km) from the epicenter. Body-wave magnitude determines the magnitude from the amplitude of the body wave at 1 Hz or with a period of 1 second, and M_S from the amplitude at 0.05 Hz or with period close to 20 seconds. Another popular measure of the size of an earthquake used by seismologists is the moment magnitude, M_W, because it basically follows the theory of focal mechanisms. Moment magnitude is defined in terms of the seismic moment, which is the product of three factors: the area of the rupture surface, the average slip, and the rigidity modulus of the rock mass at the hypocenter.

Magnitude on the Richter scale is expressed in whole numbers and decimal fractions. Each whole number step of magnitude on the scale represents an increase of 10 times in the measured wave amplitude of an earthquake. Thus, the amplitude of an 8.0 magnitude earthquake is not twice as large as a shock of magnitude 4.0 but 10,000 times as large. However, the amount of energy released, as shown in Table A.2, increases even faster - by a factor of about 30 per one step of the scale.

The Richter magnitudes commonly cited in the news media and among engineers are M_L for earthquakes with M_L less than 6.5 and M_S for earthquakes with M_S greater than 6.5. Moment magnitudes are approximately the same as the commonly cited Richter magnitudes for earthquakes with M_W less than 8.0.

Earthquakes with magnitude of about 2.0 or less are not commonly felt by people. Events with magnitudes of about 4.5 or greater are strong enough to be recorded by sensitive seismographs all over the world. Many investigators have stated that magnitude 5.5 may be the lowest threshold for earthquake-induced liquefaction.

APPENDIX A

TABLE A.2
Relationship Between the Richter Scale Magnitude and the Amount of Energy Released (Lindh, 1990; Geotechnical News, 1990)

Magnitude	Potential Energy Released (Millions of Ergs)	Energy Equivalence
-2	$6x10^{2}$	100 watt light bulb left on for a week.
-1	$2x10^{4}$	Smallest earthquakes detected.
0	$6x10^{5}$	Seismic waves from 1 lb. (0.45 kg) of explosives.
1	$2x10^{7}$	A two-ton truck traveling at 75 mph (120 km per hour).
2	$6x10^{8}$	
3	$2x10^{10}$	Smallest earthquakes commonly felt.
4	$6x10^{11}$	Seismic waves from 1,000 tons (900 metric ton) of explosives.
5	$2x10^{13}$	
6	$6x10^{14}$	1988 Quebec (Magnitude=6) Hiroshima atom bomb explosion (Magnitude=6.3)
7	$2x10^{16}$	1886 Charleston, South Carolina (Magnitude=7.3) 1964 Niigata, Japan (Magnitude=7.5)
8	$6x10^{17}$	1811-1822 New Madrid, Missouri (Magnitude=8.5) 1906 San Francisco and 1964 Anchorage (Magnitude=8.3) 1960 Chile (Magnitude=8.9)
9	$2x10^{19}$	1964 Alaska (Magnitude=9.2)
10	$6x10^{20}$	

APPENDIX B – EXAMPLE PROBLEM
US CUSTOMARY UNITS

Example Problem for Evaluating the Liquefaction Potential and for Estimating the Earthquake-Induced Settlement of Soil Deposits Under Level Ground Conditions

A soil deposit consisting of four layers with different properties listed below is subjected to ground shaking by a magnitude 6.0 earthquake.

Layer No.	Depth (ft.)	Soil Type	Unit Weight (pcf)	Ave. NYS Penetration Resistance (blows/ft.)	Fines Content (%)	PI (%)
1	0-6.5	Gravelly Sand	100	15	< 5	--
2	6.5-20	Sandy Silt, Clayey	115	10	35	10
3	20-30	Silty Sand	115	5	15	--
4	30-42	Sandy Silt	115	15	15	--

Assuming that:

1. Maximum Horizontal Acceleration = 0.15g
2. Energy Ratio of the NY State Penetration Test, in percent = 50
3. Water table is 7 ft. below the ground surface.
4. Gradation curves for all soil layers fall within Tsuchida's (1970) boundaries for "most liquefiable Soil" shown in Figure 9.

Which layers are vulnerable to liquefaction?

Layer No. 1

Since this layer of soil is above the ground water table, liquefaction is not expected to occur.

Layer No. 2

Determine the Earthquake-Induced Shear Stress Ratio

From Eq (4), $\tau_{av} / \sigma_o' = 0.65 \cdot (a_{max} / g) \cdot (\sigma_o / \sigma_o') \cdot Y_d$

$a_{max} = 0.15g$

σ_o' at mid-layer $= (6.5)(100) + (6.75)(115-62.4)$

$= 1005$ psf

From page 29, $Y_d = 1 - \frac{(13.25)(0.1)}{35} = 0.96$

σ_o at mid-layer $= 6.5(100) + 6.75(115)$

$= 1426$ psf

$$(\tau_{av} / \sigma_o')_{induced} = (0.65) \cdot (0.15g / g) \cdot (1426 / 1005) \cdot (0.96)$$
$$= 0.13$$

Estimate the Shear Stress Ratio Requird to Cause Liquefaction

$N_{NY} = 10$
$ER_m = 50$
$\sigma_o' = 1005$ psf
$C_N = (1005/2000)^{-1/2} = 1.41$

From Eq (5), $(N_1)_{60} = (1.29)\, C_N \cdot ER_m \cdot (N_{NY} /60) =$
$= (1.29)(1.41)(50)(10)/(60) = 15$

For an earthquake magnitude of 6.0, and fines content of 35%, from Figure 16,

$$(\tau_{av} / \sigma_o')_{req.} = 0.32$$

Considering the effect of soil plasticity by following Step e of Sec. 3.2.1.: Given fines content=35% and PI= 10%, ß=1.1 from Figure 17. Correct the shear stress ratio required to cause liquefaction to

$$(\tau_{av} / \sigma_o')_{req.} = (0.32) \cdot (1.1) = 0.35$$

Factor of Safety against liquefaction = (0.35 / 0.13) = 2.17 > 1.1

Therefore, layer No. 2 is nonliquefiable.

Layer No. 3

Determine the Earthquake-Induced Shear Stress Ratio

σ_o' at mid-layer = (6.5)(100)+(13.5)(115-62.4)+(5)(115-62.4)
= 1623 psf

σ_o at mid-layer = (6.5)(100)+(13.5)(115)+(5)(115)
= 2778 psf

$Y_d = 1 – ((30)(0.1))/ 35 = 0.91$

$$(\tau_{av} / \sigma_o')_{induced} = (0.65) \cdot (0.15g / g) \cdot (2778 / 1623) \cdot (0.91)$$
$$= 0.15$$

Estimate the Shear Stress Ratio Required to Cause Liquefaction

$\sigma_o' = 1623$ psf

$C_N = (1623/2000)^{-1/2} = 1.1$

$N_{NY} = 5$

$(N_1)_{60} = (1.29)(1.1)(50)(5)/(60) = 6$

From Figure 15, for earthquake magnitude at 6.0 and fines content of 15%,

$(\tau_{av} / \sigma_o')_{req.} = 0.14$

Factor of Safety against Liquefaction

F.S. = 0.14 / 0.15 = 0.93 <1.1

Layer No. 3 is potentially liquefiable.

Layer No. 4

Determine the Earthquake-Induced Shear Stress Ratio

σ_o' at mid-layer = (6.5)(100)+(13.5)(115-62.4)+(10)(115-62.4)+(6)(115-62.4)
= 2202 psf

σ_o at mid-layer = (6.5)(100)+(29.5)(115) = 4043 psf

From Figure 13, $Y_d = 0.87$

$$(\tau_{av} / \sigma_o')_{induced} = (0.65) \cdot (0.15g / g) \cdot (4043 / 2202) \cdot (0.87)$$
$$= 0.16$$

Estimate the Shear Stress Ratio Required to Cause Liquefaction

$\sigma_o' = 2202$ psf

$C_N = (2202/2000)^{-}$ = 0.95

$N_{NY} = 15$

$(N_1)_{60} = (1.29)(0.95)(50)(15)/(60)$

$= 15$

From Figure 15, for an earthquake magnitude of 6.0 and fines content of 15%,

$$(\tau_{av} / \sigma_o')_{req.} = 0.29$$

Factor of Safety against Liquefaction

F.S = 0.29/ 0.16 = 1.81 > 1.1

Layer No. 4 is nonliquefiable.

In summary, only layer No. 3 is vulnerable to liquefaction.

Estimation of the Earthquake Induced Settlement

Since only Layer No. 3 is vulnerable to liquefaction and all other soil layers have a safety factor greater than 1.25, therefore, estimate the settlement contributed by Layer No. 3 only.

Correct the previously calculated earthquake induced stress ratio in Layer No.3 to the equivalent stress ratio that would be induced by an M=7.5 event:

From Eq(6) and Figure 22, $\gamma_m = 1.32$

$$(\tau_{av} / \sigma_o')_{induced\ at\ M=7.5} = (0.16)(1/1.32) = 0.12$$

From Page B-3, $(N_1)_{60} = 6$, and from Figure 21, $\varepsilon_V = 3.3\%$

Layer No.3 is 10 ft. thick, therefore

Settlement = (3.3/100)(10)(12) = 4 in.

APPENDIX B – EXAMPLE PROBLEM
INTERNATIONAL SYTEM OF UNITS

Example Problem for Evaluating the Liquefaction Potential and for Estimating the Earthquake-Induced Settlement of Soil Deposits Under Level Ground Conditions

A soil deposit consisting of four layers with different properties listed below is subjected to ground shaking by a magnitude 6.0 earthquake.

Layer No.	Depth (m)	Soil Type	Unit Weight (kN/m^3)	Ave. NYS Penetration Resistance (blows/0.3 m)	Fines Content (%)	PI (%)
1	0-2	Gravelly Sand	16	15	< 5	--
2	2-6	Sandy Silt, Clayey	18	10	35	10
3	6-10	Silty Sand	18	5	15	--
4	10-13	Sandy Silt	18	15	15	--

Assuming that:

1. Maximum Horizontal Acceleration = 0.15g
2. Energy Ratio of the NY State Penetration Test, in percent = 50
3. Water table is 2 m below the ground surface.
4. Gradation curves for all soil layers fall within Tsuchida's (1970) boundaries for "most liquefiable Soil" shown in Figure 9.

Which layers are vulnerable to liquefaction?

Layer No. 1

Since this layer of soil is above the ground water table, liquefaction is not expected to occur.

Layer No. 2

Determine the Earthquake-Induced Shear Stress Ratio

From Eq (4), $\tau_{av} / \sigma_o' = 0.65 \cdot (a_{max} / g) \cdot (\sigma_o / \sigma_o') \cdot Y_d$

$a_{max} = 0.15g$

σ_o' at mid-layer $= (2)(16) + (2)(18-9.8)$

$= 48.4\ kN/m^2$

From page 29, $Y_d = 1 - \frac{(4)(0.1)}{10.67} = 0.96$

σ_o at mid-layer $= 2(16) + 2(18)$

$= 68\ kN/m^2$

$$(\tau_{av} / \sigma_o')_{induced} = (0.65) \cdot (0.15g / g) \cdot (68 / 48.4) \cdot (0.96)$$
$$= 0.13$$

Estimate the Shear Stress Ratio Requird to Cause Liquefaction

$N_{NY} = 10$
$ER_m = 50$
$\sigma_o' = 48.4$ kN/m^2
$C_N = (48.4/95.76)^{-1/2} = 1.41$

From Eq (5), $(N_1)_{60} = (1.29)\, C_N \cdot ER_m \cdot (N_{NY} /60) =$
$= (1.29)(1.41)(50)(10)/(60) = 15$

For an earthquake magnitude of 6.0, and fines content of 35%, from Figure 16,

$$(\tau_{av} / \sigma_o')_{req.} = 0.32$$

Considering the effect of soil plasticity by following Step e of Sec. 3.2.1.: Given fines content=35% and PI= 10%, ß=1.1 from Figure 17. Correct the shear stress ratio required to cause liquefaction to

$$(\tau_{av} / \sigma_o')_{req.} = (0.32) \cdot (1.1) = 0.35$$

Factor of Safety against liquefaction = (0.35 / 0.13) = 2.17 > 1.1

Therefore, layer No. 2 is nonliquefiable.

Layer No. 3

Determine the Earthquake-Induced Shear Stress Ratio

σ_o' at mid-layer = (2)(16)+(4)(18-9.8)+(2)(18-9.8)
= 81.2 kN/m^2

σ_o at mid-layer = (2)(16)+(4)(18)+(2)(18)
= 140 kN/m^2

$Y_d = 1 – ((8)(0.1))/ 10.67 = 0.93$

$$(\tau_{av} / \sigma_o')_{induced} = (0.65) \cdot (0.15g / g) \cdot (140 / 81.2) \cdot (0.93)$$
$$= 0.16$$

Estimate the Shear Stress Ratio Required to Cause Liquefaction

$\sigma_o' = 81.2$ kN/m^2

$C_N = (81.2/95.76)^{-1/2} = 1.09$

$N_{NY} = 5$

$(N_1)_{60} = (1.29)(1.09)(50)(5)/(60) = 6$

From Figure 15, for earthquake magnitude at 6.0 and fines content of 15%,

$(\tau_{av} / \sigma_o')_{req.} = 0.14$

Factor of Safety against Liquefaction

F.S. = 0.14 / 0.16 = 0.88 <1.1

Layer No. 3 is potentially liquefiable.

Layer No. 4

Determine the Earthquake-Induced Shear Stress Ratio

σ_o' at mid-layer = (2)(16)+(4)(18-9.8)+(4)(18-9.8)+(1.5)(18-9.8)
= 109.9 kN/m^2

σ_o at mid-layer = (2)(16)+(9.5)(18) = 203 kN/m^2

From Figure 13, $Y_d = 0.87$

$$(\tau_{av} / \sigma_o')_{induced} = (0.65) \cdot (0.15g / g) \cdot (203 / 109.9) \cdot (0.87)$$
$$= 0.16$$

Estimate the Shear Stress Ratio Required to Cause Liquefaction

$\sigma_o' = 109.9$ kN/m^2

$C_N = (109.9/95.76)^{-}$ = 0.93

$N_{NY} = 15$

$(N_1)_{60} = (1.29)(0.93)(50)(15)/(60)$

$= 15$

From Figure 15, for an earthquake magnitude of 6.0 and fines content of 15%,

$$(\tau_{av} / \sigma_o')_{req.} = 0.29$$

Factor of Safety against Liquefaction

$$F.S = 0.29/ 0.16 = 1.81 > 1.1$$

Layer No. 4 is nonliquefiable.

In summary, only layer No. 3 is vulnerable to liquefaction.

Estimation of the Earthquake Induced Settlement

Since only Layer No. 3 is vulnerable to liquefaction and all other soil layers have a safety factor greater than 1.25, therefore, estimate the settlement contributed by Layer No. 3 only.

Correct the previously calculated earthquake induced stress ratio in Layer No.3 to the equivalent stress ratio that would be induced by an M=7.5 event:

From Eq(6) and Figure 22, $\gamma_m = 1.32$

$$(\tau_{av} / \sigma_o')_{induced\ at\ M=7.5} = (0.16)(1/1.32) = 0.12$$

From Page B-7, $(N_1)_{60} = 6$, and from Figure 21, $\varepsilon_V = 3.3\%$

Layer No.3 is 4 m thick, therefore

Settlement = (3.3/100)(4)(1000) = 132 mm

APPENDIX C – EXAMPLE PROBLEM
US CUSTOMARY UNITS

Example Problem for Analyzing the Stability of an Embankment Against Flow Failure

A seven-meter-high embankment sloping at 1 vertical on 2 horizontal is constructed over a saturated soil deposit consisting of three layers with properties listed below. If the site is stricken by an M=6.0 earthquake and, both silty sand and sandy silt layers reach the state of initial liquefaction during shaking, calculate the factor of safety of the embankment against flow failure.

Layer No.	**Depth* (ft.)**	**Soil Description**	**Total Unit Weight of Soil (pcf)**	**Ave. $(N_1)_{60}$ (blows/ft.)**	**Fines Content (%)**	**Undrained Shear Strength, S_u (psf)**
		Embankment Material	120	20	30	940
1	0-6.5	Silty Sand	115	6	10	--
2	6.5-16.5	Sandy Silt	120	10	30	--
3	16.5-30	Clayey Silt	120	--	--	1460

* measured from the base of the embankment

Perform a conventional static stability analysis considering both possibilities of wedge and circular types of failure. Assuming that no loss of strength takes place in both embankment material and heavily overconsolidated clayey silt during the shaking, therefore, use their undrained shear strengths in the stability analysis, i.e., S_u=940 psf for the embankment material and S_u=1460 psf for clayey silt. According to Sec. 3.3, the average residual shear strengths for silty sand and sandy silt layers can be estimated as follows:

	(1)** $\Delta(N_1)_{60}$ (b/ft.)	(2) Ave. $(N_1)_{60}$ (b/ft.)	(3)=(1)+(2) Equivalent Clean Sand $(N_1)_{60}$ (b/ft.)	(4)*** Ave. residual Shear Strength (psf)
Silty Sand	1.0	6.0	7.0	165
Sandy Silt	2.4	10.0	12.4	500

** - From Fig. 20

*** - From Fig. 19

The minimum factor of safety against flow slide from an XSTABL run is 1.22 and greater than 1.0. Therefore, it is assumed that the embankment will be stable during and after the seismic shaking.

APPENDIX C – EXAMPLE PROBLEM
INTERNATIONAL SYSTEM OF UNITS

Example Problem for Analyzing the Stability of an Embankment Against Flow Failure

A seven-meter-high embankment sloping at 1 vertical on 2 horizontal is constructed over a saturated soil deposit consisting of three layers with properties listed below. If the site is stricken by an M=6.0 earthquake and, both silty sand and sandy silt layers reach the state of initial liquefaction during shaking, calculate the factor of safety of the embankment against flow failure.

Layer No.	**Depth* (m)**	**Soil Description**	**Total Unit Weight of Soil (kN/m^3)**	**Ave. $(N_1)_{60}$ (blows/0.3 m)**	**Fines Content (%)**	**Undrained Shear Strength, S_u (kPa)**
		Embankment Material	19	20	30	45
1	0-2	Silty Sand	18	6	10	--
2	2-5	Sandy Silt	19	10	30	--
3	4-10	Clayey Silt	19	--	--	70

* measured from the base of the embankment

Perform a conventional static stability analysis considering both possibilities of wedge and circular types of failure. Assuming that no loss of strength takes place in both embankment material and heavily overconsolidated clayey silt during the shaking, therefore, use their undrained shear strengths in the stability analysis, i.e., S_u=45 kPa for the embankment material and S_u=70 kPa for clayey silt. According to Sec. 3.3, the average residual shear strengths for silty sand and sandy silt layers can be estimated as follows:

	(1)** $\Delta(N_1)_{60}$ (b/0.3 m)	(2) Ave. $(N_1)_{60}$ (b/0.3 m)	(3)=(1)+(2) Equivalent Clean Sand $(N_1)_{60}$ (b/0.3 m)	(4)*** Ave. residual Shear Strength (kPa)
Silty Sand	1.0	6.0	7.0	8
Sandy Silt	2.4	10.0	12.4	24

** - From Fig. 20
*** - From Fig. 19

The minimum factor of safety against flow slide from an XSTABL run is 1.22 and greater than 1.0. Therefore, it is assumed that the embankment will be stable during and after the seismic shaking.